8-2017

Metabolic Regulation by Stress Mediators in Fetal Ovine Skeletal Muscle and Adult Bovine Myoblasts

Elena Marie Merrick
University of Nebraska-Lincoln, elena.merrick@huskers.unl.edu

METABOLIC REGULATION BY STRESS MEDIATORS IN FETAL OVINE SKELETAL MUSCLE AND ADULT BOVINE MYOBLASTS

by

Elena Marie Merrick

A THESIS

Presented to the Faculty of

The Graduate College at the University of Nebraska

In Partial Fulfillment of Requirements

For the Degree of Master of Science

Major: Animal Science

Under the Supervision of Professor Dustin T. Yates

Lincoln, Nebraska

August 2017

METABOLIC REGULATION BY STRESS MEDIATORS IN FETAL OVINE SKELETAL MUSCLE AND ADULT BOVINE MYOBLASTS

Elena Marie Merrick M.S.

University of Nebraska, 2017

Advisor: Dustin T. Yates

Our objective was to determine the effect of stress mediators such as inflammatory cytokines and β adrenergic agonists on developing skeletal muscle. Fetal sheep exposed to chronic maternal inflammation had decreased skeletal muscle glucose oxidation rates when stimulated with insulin or TNFα. In addition, activation of Akt by insulin was decreased after maternal inflammation when compared to controls and there were not differences in skeletal muscle fiber type ratios between the two treatment groups. This indicates that maternal inflammation does not affect overall oxidative capacity in the developing fetus, but rather insulin signaling pathways are disrupted.

We sought to determine whether the metabolic response to β adrenergic and insulin stimulation previously shown in mature skeletal muscle is a phenotypic trait passed to the mature muscle from developing muscle stem cells. Bovine myoblasts were differentiated in media containing either β1 adrenergic agonist +/- insulin or β2 adrenergic agonist +/- insulin. Glucose oxidation was increased in the myoblasts simulated by β2 adrenergic agonist compared to myoblasts stimulated by β1 adrenergic agonists suggesting that the β2 adrenergic agonist is more effective at enhancing glucose metabolic efficiency than the β1 adrenergic agonist. Furthermore, we determined that when stimulated by β2 adrenergic agonist and insulin, myoblasts had decreased glucose

oxidation rates compared to insulin alone. This is opposite of the effects seen in a similar study conducted utilizing mature skeletal muscle, indicating that this response is not necessarily derived from the muscle stem cell.

In a final study, we evaluated mitochondrial respiration rate in bovine myoblasts from cows that had been classified as having either High or Low concentrations of androstenedione (A4) in their follicular fluid. Calves born to cows classified as High A4 had increased weaning weights compared to calves born to cows classified as Low A4. By performing a mitochondrial stress test using an XF-96 Seahorse Bioanalyzer, we were able to measure cellular respiration. We hypothesized that myoblasts from the High A4 cows would have enhanced metabolic efficiency compared to the Low A4 cows. However, we found no differences in mitochondrial oxidation rates among treatments but did find a tendency ($P = 0.1$) for muscle stem cells from High A4 cows in the absence of insulin and from Low A4 cows when insulin was present to have increased rates of glycolysis. This indicates that the enhanced growth efficiency of the calves born to the High A4 cows is likely due to a different biological mechanism.

Acknowledgements

First and foremost, I would like to thank my advisor Dr. Dustin Yates for giving me the opportunity to work in his lab. I did not have a research background coming into graduate school so I am beyond thankful to have been given the chance to develop my skills and to gain confidence in myself over the last two years.

I would also like to thank my committee members, Dr. Andrea Cupp and Dr. Jessica Petersen for their guidance and support throughout my Master's program. I really enjoyed learning from Dr. Cupp. She is a wonderful teacher and I am glad I was able to take her Endocrinology class. I was fortunate enough to have the opportunity to work on a collaborative project with Dr. Petersen. She is a lot of fun to work with and her witty sense of humor definitely helped us get through some long days.

While I greatly appreciate all the hard work that my lab members have put into helping me with these projects, I would like to give a special shout out to our lab technician, Kristin Beede. I had absolutely no lab experience when I first started graduate school so I know that it took a lot of patience and understanding to teach me all of the protocols that I used for these projects.

I never would have made it this far without my better half, Cody Stout. He is the best friend I could have ever asked for. He has moved all over the place for me because he understands how much my education means to me. I'll never be able to express my appreciation for his unconditional love and support.

If not for my amazing parents, I would not be the person I am today. I will never be able to repay them for the tremendous amount of support they have offered (both emotionally and financially!). I honestly don't think either one of them ever missed a single track or cross country race when I was growing up. To this day, they will always be a comforting conversation at the end of a long day. My mom has always encouraged me to try new things and to visit new places while my dad has always kept me grounded, making sure I always remember where home is.

My greatest inspiration in my pursuit of a career in Animal Science has been my family, a few members in particular that deserve recognition. My sister, Christina, and I share the same love for animals. Being my big sister, she has always been someone I look up to. I appreciate her willingness to let me help take care of her animals when I was growing up. I spent a lot of time at her house playing with her dogs and riding her horses. My grandma, Reva, was one of the smartest women I ever knew. She definitely passed on her love of learning to me. I miss spending my summers with her, soaking up everything she taught me about life, history, and science. Finally, I would like to extend my appreciation to my Aunt Terri and Uncle Craig. If it hadn't been for all of those summers spent at their ranch in Wyoming riding horses and helping check cows, I may never have found my niche working with livestock.

Finally, I would not have made it through graduate school without my friends. Graduate school brought me to some of the best friends I have ever had. From our "Wednesday night shenanigans" to just having someone to hang out with during a late night in the lab, I am so thankful for the support and laughter these wonderful people have brought me.

Table of Contents

Chapter 1: Literature Review

Chapter 1

Literature Review

Introduction

Intrauterine Growth Restriction

Placental insufficiency can be defined as a smaller or functionally stunted placenta that limits the flow of nutrients from mother to fetus, leading to intrauterine growth restriction (IUGR) (Molteni et al., 1978; Marconi et al., 2006; Alisi et al., 2011). In the United States, IUGR is clinically defined as birth weight that falls below the 10^{th} percentile for an infant's gestational age (Morrison, 2008). Infants born small for gestational age (SGA) have an increased risk of developing metabolic syndrome later in life, abnormal partitioning of dietary nutrients (Brodsky and Christou, 2004), and an increase in perinatal and neonatal morbidity and mortality (Pollack and Divon, 1992; Brodsky and Christou, 2004; Tuuli et al., 2011).

Impact of IUGR on Life Quality

Perinatal Morbidity and Mortality

Developmental adaptations due to IUGR have detrimental effects on infants during the perinatal period. This includes increased risk of hypoglycemia, hypothermia, chronic lung disease, and impairment of renal function (Chiswick, 1985). In addition, many neonatal complications resulting from IUGR lead to death.

Childhood and Adult Disease

IUGR also increases the risk of developing metabolic dysfunction, which can substantially reduce the quality of life in humans because it leads to multiple health issues. IUGR-induced metabolic dysfunction has been associated with an increased risk of developing cardiovascular disease, type II diabetes, and predisposition to central obesity; each of these factors increase the risk of morbidity and mortality (Gallagher et al., 2011). Obese patients due to metabolic dysfunction can experience fatigue and an increase in appetite stimulation, both of which contribute to further weight gain (Gallagher et al., 2011). Furthermore, patients with central obesity have a higher risk of developing fatty liver disease than patients with lower body fat (Grundy, 2000). Studies have also shown that patients with obesity are more likely to develop certain cancers including colon, breast, and prostate cancer (Grundy, 2000). Patients with metabolic dysfunction require aggressive, long-term medical treatment in order to manage the risk of chronic diseases such as cardiovascular disease and type II diabetes (Gallagher et al., 2011). In fact, metabolic complications of diabetes costs an estimated $2.4 billion in annual direct medical expenses (Kitabchi et al., 2009). The incidence of obesity and other conditions related to metabolic dysfunction is increasing globally and is expected to affect 40% of the world's population by 2025 (Rinaudo and Wang, 2012). As many as half of all clinical cases of metabolic disease are believed to be predisposed by IUGR (Vonnahme, 2012). By understanding the underlying mechanisms, the incidence of metabolic syndrome could be reduced in the future.

Impact of IUGR on Livestock Efficiency

In meat animals, a high proportion of muscle is critical because meat is the profitable product (Irshad et al., 2013). However, IUGR results in a decrease in muscle

growth due to adaptive fetal programming in response to restriction of nutrients. In fact, nutrient restriction from early to mid-gestation has been shown to reduce muscle fiber number in fetuses (Zhu et al., 2004). Furthermore, IUGR-induced low birth weight in livestock species can lead to increased perinatal mortality due to reduced vigor (Greenwood and Bell, 2002). Skeletal muscle makes up about 40% of the body's mass and plays a critical role in metabolism (DeFronzo et al., 1981). Consequently, as IUGR-induced low birth weight offspring mature, these animals develop a greater fat-to-muscle ratio and have reduced lean muscle mass (Yates et al., 2012), leading to a decrease in carcass quality, yield, and profit for the producer. Therefore, by understanding the underlying mechanisms linking IUGR and poor muscle growth efficiency, carcass quality and yield in low birth weight livestock could be improved, resulting in greater profit for the producer.

Metabolic Syndrome

Metabolic syndrome is a human condition defined by the clinical diagnosis of three out of the following five metabolic characteristics; insulin resistance, hypertension, central obesity, increased triglyceride concentration, and decreased high density lipoprotein concentration (Gallegher et al, 2011). This manuscript focuses on insulin resistance, central obesity, and hypertension.

Insulin Resistance

Clinically defined as a reduction in biological response to insulin secretion (Cefalu, 2001), insulin resistance is a known constituent of metabolic syndrome that is often a result of stress-induced adaptive fetal programming (Hales and Barker, 2001;

Gallagher et al., 2011). Insulin resistance manifests to type II diabetes when insulin is no longer secreted at a high enough concentration to compensate for the lack of insulin action due to reduced sensitivity (Reaven, 2005). Metabolic adaptations that contribute to the development of insulin resistance in IUGR individuals include reduced skeletal muscle mass and disruptions in insulin signaling pathways (Ozanne et al., 2005). Fetal stress responses result from placental insufficiency and mediate nutritional thrift in order to spare available nutrients for the most critical tissues to aid fetal survival. However, when the IUGR individual is born into an environment where nutritional thrift is no longer necessary and the mechanism has been programmed, insulin resistance is more likely to develop due to typical calorie intake combined with thrifty energy expenditure (Hales and Barker, 2001).

Central Obesity

Another characteristic of metabolic syndrome is central obesity. Obesity is clinically defined as body mass index (BMI) >30 kg/m^2 (Gallagher et al., 2011) as opposed to clinically overweight which is defined as BMI >27.8 for males and >27.3 for females (Van Itallie, 1985). Central obesity, or excessive truncal fat (Klein et al., 2007), is indicative of adaptive fetal programming that disrupts metabolic function. IUGR-born infants experience postnatal "catch-up" growth (Vaag, 2009), a period during early life in which rapid weight gain occurs (Law et al., 2002). However, this has negative effects on metabolic health later in life due to accelerated weight gain from fat deposition rather than skeletal muscle accretion (Vaag, 2009). This is problematic in livestock production as well, since animals develop greater fat-to-muscle body composition, resulting in lower yield and meat quality (Irshad et al., 2013).

Hypertension

Up to 85% of patients with metabolic dysfunction develop hypertension (Duvnjak et al., 2008), which is clinically defined as blood pressure of ≥140/90 mmHg systolic over diastolic, respectively (Gallagher et al., 2011). Hyperinsulinemia resulting from insulin resistance elevates blood pressure, leading to sodium retention and volume expansion (Duvnjak et al., 2008). Obese individuals tend to have increased blood pressure, also leading to volume expansion and an increase in cardiac output (Grundy, 2000). Hypertension due to insulin resistance and obesity further manifests into vascular damage (Duvnjak et al., 2008), cardiovascular disease, stroke, heart failure, and renal failure (Grundy, 2000).

The "Thrifty Phenotype Hypothesis"

Adaptive Fetal Programming

About 25 years ago, David J.P. Barker first published his *Thrifty Phenotype Hypothesis* which described the epidemiological link between individuals who are born small for gestational age (SGA) and their increased risk of developing metabolic syndrome later in life (Hales et al., 1991; Hales and Barker, 1992; Barker et al., 1993). *The Thrifty Phenotype Hypothesis* suggests that the link between stress induced low birth weight and the increased risk of developing metabolic syndrome results from fetal adaptations to stress, resulting from a decrease in available nutrients that lead to programmed alterations in glucose metabolism (Hales and Barker, 2001). Fetuses are extremely responsive to their environment which can greatly influence their

development, and developmental plasticity is reduced drastically after birth (Gluckman and Hanson, 2004). Development of thrifty metabolic rates leads to more dietary nutrients being directed toward storage as fat rather than being used for muscle accretion or energy production. (Barker, 1998; Hales and Barker, 2001) Thrifty adaptive programming is beneficial during gestation, however, it greatly increases the risk of developing metabolic diseases in childhood and adulthood (Yates et al., 2012) including metabolic syndrome (Barker et al., 1993). This is due to the inability for IUGR-born individuals to cope with a different nutritional environment after birth (Rinaudo and Wang, 2012). Since the postnatal diet is typically not limited, IUGR-born individuals develop excess fat and not enough skeletal muscle due to restriction of nutrient and oxygen transport during development (Bauer et al., 1998). Epidemiological studies overwhelmingly support a link between IUGR and the increased risk of developing metabolic syndrome (Barker, 1998; Hales and Barker, 2001). In fact, IUGR-born offspring are 18-times more likely to develop metabolic syndrome than offspring born at appropriate size for gestational age (Gatford et al., 2010). However, the underlying mechanisms explaining the link between IUGR fetuses and the increased risk of developing metabolic syndrome is still unknown (Hales and Barker, 2001; Vaag, 2009).

Maternal Stressors and Fetal Stress

The most common maternal stressors associated with IUGR in humans include illness, nutritional deficiencies, and exposure to toxins during pregnancy (Rinaudo and Wang, 2012) such as the use of drugs, smoking, or alcohol. The most common maternal etiologies in livestock include environmental stressors such as heat, cold, or altitude stress (Yates et al., 2011) as well as nutritional stress (Vonnahme, 2012). All of these

stressors can cause placental stunting by reducing uterine blood flow (Bell et al., 1987) (Figure1). Changes in placental vasculature caused by placental stunting limit the umbilical vein and fetal artery's ability to receive oxygen and nutrients (Greenwood and Bell, 2002; Regnault et al., 2007; Vonnahme, 2012). This results in a chronically hypoxic and hypoglycemic fetus later in gestation (Greenwood and Bell, 2002). As fetal hypoxemia and hypoglycemia worsen, hypercatecholaminemia and hypoinsulinemia develop in turn, since adrenal secretion of catecholamines work towards maintaining fetal glucose supply by suppressing insulin secretion (Leos et al., 2010). The comprehensive adaptations due to fetal stress are still unknown, but understanding the mechanisms involved is the first step to finding a way to prevent or treat the effects of maternal stress on the developing fetus.

Characteristics of IUGR Pathology

Sheep as a Model for Placental Insufficiency-Induced IUGR

Using animals as a model for biomedical research is advantageous because it allows researchers to assess the effects of a particular stress applied over a certain time period in a more controlled setting. Rodent and sheep models are the most common models used for fetal biomedical research. The rodent model has advantages such as lower cost and rapid gestation period. However, sheep physiology more closely resembles human physiology, including metabolic function, nutrient transport, and developmental milestones and critical periods (Barry and Anthony, 2008). Furthermore, the ewe can be selected for one fetus as opposed to a litter of offspring such as rodents

(Green et al., 2011; Rinaudo and Wang, 2012). Sheep also allow researchers to monitor placental exchange as well as fetal physiology in utero in the conscious animal due to the ability of the fetus to tolerate catheterization of fetal blood vessels that allows frequent, real-time sampling from the conscious animal in utero. These characteristics make the pregnant sheep a valuable model for human biomedical research (Barry and Anthony, 2008; Green et al., 2011).

The Role of Skeletal Muscle in IUGR Adaptations

Sufficient skeletal muscle mass plays an important role in glucose homeostasis and the metabolic health of an individual. Skeletal muscle makes up ~40% of the body's mass (Yates et al., 2012) and accounts for greater than 80% of all insulin stimulated glucose utilization (DeFronzo et al., 1981) and thus skeletal muscle plays a major role in glucose homeostasis (Yates et al., 2012). However, placental insufficiency is known to cause a reduction in fetal muscle mass due to the disruption of myogenesis (Yates et al., 2012; Yates et al., 2014; Yates et al., 2016). This reduction in muscle mass carries into adulthood and is known to have an impact on muscle strength (Inskip et al., 2007; Ylihärsilä et al., 2007). Furthermore, there are strong correlations between IUGR, insufficient muscle mass, and the development of insulin resistance, which leads to the development of type II diabetes and the metabolic syndrome (Hales et al., 1991; Hales and Barker, 2001). However, the origins of decreased muscle growth and metabolic dysfunction in IUGR fetuses and IUGR-born offspring at the cellular level are not presently understood, but the characterized pathologies are described in Figure 2.

Effects of IUGR on Skeletal Muscle Mass

IUGR results in asymmetric growth due to disproportional reduction of muscle mass and an increase in adipose tissue deposition after birth (De Blasio et al., 2007) because skeletal muscle growth continues to be much slower in individuals born IUGR. Ultrasonic measurements of IUGR fetuses show reduced muscle mass when compared to non IUGR fetuses (Galan et al., 1999). Furthermore, IUGR individuals are not only likely to have impaired muscle growth capacity, but also store more energy in adipose tissue as a result of thrifty programming. Having less muscle mass is an advantage for these fetuses because skeletal muscle is a major consumer of glucose, which the fetus requires for normal development and function of neural, cardiac, and endocrine tissues (Klip and Pâquet, 1990).

Myoblast/Myofiber Dynamics

During the early development of muscle, mononuclear muscle stem cells called myoblasts proliferate, differentiate, and fuse into multinuclear myofibers (Yates et al., 2012). During early gestational development, embryonic myoblasts fuse and form primary myofibers which provide scaffolding for myoblast facilitated formation of secondary myofibers (Yates et al., 2012; Brown, 2014) (Figure 3). Secondary myogenesis occurs during mid-gestation. This involves proliferation of the fetal myoblasts which is followed by expression of muscle regulatory factors (MRFs). Myofibers grow by increasing in diameter and length, in a process known as hypertrophy. Hypertrophy is mediated by activation and fusion of satellite cells with existing fibers and is the only form of muscle growth after birth, since myofiber numbers can no longer increase (Allen and Rankin, 1990). Myogenic markers such as Pax7, MyoD, and Myogenin can be used to identify the stage at which myoblasts are at in their cycle. IUGR can have a negative

impact on muscle development by disrupting this process, however the molecular mechanisms remain to be understood. Pax7 is present in both fetal and postnatal skeletal muscle (Hutcheson et al., 2009) and is expressed prior to differentiation (Zammit et al., 2006). During proliferation, myoblasts express MyoD (Gillespie et al., 2009) and continue to express as they exit the cell cycle and enter terminal differentiation (L'honore et al., 2007). This leads into an increase in expression of Myogenin, the regulatory factor that promotes fusion of myoblasts into myofibers (Edmondson and Olson, 1989).

Effects of IUGR on Skeletal Muscle Metabolic Rates

IUGR individuals have a higher risk of developing metabolic dysfunction than non IUGR individuals. IUGR fetuses have altered metabolic rates because it allows them to survive a harsh uterine environment. Insulin stimulated glucose uptake rate is greatest in type I muscle fibers because this fiber type has the greatest insulin sensitivity (Lillioja et al., 1987). IUGR fetuses are known to have diminished type I fiber to type II fiber ratios, leading to unfavorable consequences in glucose homeostasis (Yates et al., 2016). This insulin resistance leads to a loss of glucose homeostasis in adulthood (Ozanne et al., 2005). Furthermore, a reduction in type I muscle fibers is known to reduce glucose oxidation rates (Yates et al., 2012). Additionally, IUGR fetuses are characterized by hyperlactatemia (Jones and Ritchie, 1978; Maeda and Koos, 2009). Increased concentrations of catecholamines and acute hypoxemia during fetal stress causes a shift in metabolism from aerobic to anaerobic metabolism, resulting in increased lactate production (Limesand et al., 2007; Yates et al., 2012; Brown et al., 2015).

Type I Muscle Fibers Are Most Impacted by IUGR

In healthy individuals and livestock (Wilson et al., 1992), there is a natural shift from type II to type I muscle fibers throughout late gestation and in the first few months of life, however, IUGR may inhibit this shift and thus decrease metabolic plasticity (Yates et al., 2016). IUGR is predictive of a disproportional decrease in skeletal muscle mass throughout life. This is especially evident in muscles that are composed of type I muscle fibers, including soleus (De Blasio et al., 2007). Type I muscle fibers generally have the highest oxidative capacity, larger amounts of GLUT4, increased β adrenergic receptors which make them more likely to be impacted by the chronic stress response (Yates et al., 2012), and are especially prone to insulin insensitivity (Yates et al., 2016). Thus, greater nutrient sparing results when the type I muscle fiber proportion is disproportionately reduced relative to type II. Muscle fiber number is set before birth in most species, and there is no increase in muscle fiber number once an individual is born (Zhu et al., 2006; Yates et al., 2012; Brown, 2014). It is thought that nutrient restriction to the muscle fibers is linked to the predisposition of individuals born as a result of IUGR to the development of type II diabetes (Zhu et al., 2006).

Reduced Insulin Sensitivity

IUGR causes a reduction in the offspring's insulin sensitivity, resulting in insulin resistance and eventually type II diabetes (Limesand et al., 2007). Insulin resistance is the metabolic state wherein peripheral tissues, especially skeletal muscle, have a reduced response to the effects of insulin and therefore glucose uptake rate by the cells is diminished (Dunlop et al., 2015). Skeletal muscle is most impacted by reduced insulin sensitivity because it accounts for greater than 80% of the body's insulin stimulated glucose utilization (DeFronzo et al., 1981). Insulin acts by binding to its tyrosine kinase

receptor on the cell surface, which ultimately promotes translocation of GLUT4 to the surface of the cell. Autophosphorylation of tyrosine kinase, which catalyzes the phosphorylation of IRS1 and in turn Akt, results in the regulation of glucose uptake (Saltiel and Kahn, 2001). Previous studies have shown that the expression of the insulin receptor is actually increased in IUGR fetuses (Limesand et al., 2007), which is thought to be a compensatory mechanism for the decrease in circulating fetal insulin. However, expression of the receptors was not different in IUGR versus normal birth weight offspring, indicating that insulin resistance later in life results from a downstream defect of the receptor which alters the function of GLUT4 (Dunlop et al., 2015).

Skeletal Muscle Glucose Homeostasis

IUGR Blood Glucose Concentrations

Glucose is the primary energy substrate utilized by the fetus for normal growth and metabolism (Hay, 2006) and thus the latter is dependent on fetal plasma glucose concentration. Skeletal muscle adapts in response to glucose concentration (Yates et al., 2016). In a chronically hyperglycemic condition, there is a reduction in GLUT4 as well as other insulin signaling components (Limesand et al., 2007) in skeletal muscle which correlates with the development of insulin resistance later in life (Hay, 2006; Dulloo, 2008). A reduction in GLUT4 transporters in skeletal muscle cells reduces insulin sensitivity, resulting in a continuous state of hyperglycemia in adults (Dunlop et al., 2015). In hypoglycemic conditions, insulin responsive tissues are known to adapt using mechanisms such as increased insulin action and regulation of glucose transporter

concentrations that promote glucose utilization (Limesand et al., 2007). However, glucose transporter concentrations are not different between IUGR and normal birthweight individuals later in life (Dunlop et al., 2015).

Glucose Uptake and Metabolism

Glucose uptake and glucose oxidation play independent roles in an individual's metabolic rate. Glucose uptake is when glucose molecules are brought into the cells by insulin sensitive GLUT4 and other GLUT transporters (Saltiel and Kahn, 2001; Leney and Tavaré, 2009). There are multiples types of GLUTs that have different specificities, kinetic properties, and expression profiles (Wood and Trayhurn, 2003). However, GLUT4 is insulin stimulated (Abel et al., 2001; Saltiel and Kahn, 2001). A wide variety of metabolic pathways follow glucose uptake such as glycolysis. Pyruvate is synthesized during this process. Pyruvate formed during glycolysis is oxidized to acetyl-CoA which then enters the citric acid cycle (Nelson and Cox, 2008, pg. 616). Insulin-stimulated glucose uptake and oxidation are presumed to be proportional, however, the presence of stress factors such as inflammatory cytokines may alter these metabolic functions (Cadaret et al., 2017b). In fact, IUGR fetuses are known to have lower glucose oxidative metabolism (Yates et al., 2012). By performing glucose uptake and oxidation studies, researchers are able to further their understanding of how acute and chronic stress factors change metabolic rates. Increased circulating catacholamines and decreased insulin concentrations in IUGR fetuses in concert contribute to hyperlactatemia which may be caused by reduced glucose oxidation in the skeletal muscle in order to spare glucose and oxygen for vital tissues such as the brain. Prolonged durations of skeletal muscle nutrient and oxygen deprivation causes a metabolic shift. Therefore, adaptations to fetal

catecholamine concentrations *in utero* may explain this shift from oxidative metabolism to anaerobic glycolysis (Yates et al., 2012) (Figure 4). Furthermore, anaerobic glycolysis in meat producing animals is unfavorable due to a decrease in pH caused by lactate production which is known to effect meat quality attributes including water holding capacity, color, and juiciness (Andersen et al., 2005).

Inflammatory Component of the Stress Response

Introduction to Cytokines

Pro-inflammatory cytokines such as IL-6 (Interleukin-6) and TNFα (Tumor Necrosis Factor) play a critical role in the inflammatory response of IUGR (Bartha et al., 2003). These cytokines are predominantly produced by macrophages and participate in the up-regulation of inflammatory reactions (Zhang and An, 2007). In addition to pro-inflammatory cytokines, there is another group of cytokines known as the anti-inflammatory cytokines including IL-1, IL-4, IL-10, IL-11, and IL-13. (Zhang and An, 2007). Pro-inflammatory cytokines are associated with skeletal muscle degeneration during states of chronic stress (Späte and Schulze, 2004), while anti-inflammatory cytokines are immunoregulatory molecules that regulate the response of the pro-inflammatory cytokines by inhibiting their function. The inflammatory and metabolic systems are closely linked which is advantageous under certain conditions. For example, an organism may need to redistribute its energy sources during an inflammatory response (Dionne et al., 2006). Furthermore, the pro-inflammatory cytokine TNFα is highly expressed in adipose tissue (Hotamisligil et al., 1993) and also plays a role in disrupting

insulin signaling pathways when activated (Uysal et al., 1997). Elevated concentrations of inflammatory cytokines under stressful conditions mediate proteolysis so that available amino acids provide fuel to the liver rather than skeletal muscle, resulting in an inhibition of muscle growth (Klasing and Johnstone, 1991). Therefore, inflammatory cytokines play major roles in both metabolism and muscle growth in IUGR individuals.

Cytokine Signaling

The major cytokine signaling pathways have been reviewed in detail by O'Shea et al. 2002 (Figure 5). The cytokine signaling pathway begins when inflammatory cytokines bind to homodimeric or heterodimeric receptors. These receptors bind to Janus kinases (JAKs) which phosphorylate the cytokine receptors. This phosphorylation allows signal transducers and activators of transcription (STAT) to bind. STAT is then phosphorylated and translocated to the nucleus of the cell where it binds to DNA and functions to regulate gene expression. More specifically, TNFα activates the transcription factor NFκB (Van Antwerp et al., 1996). Furthermore, cytokines can be regulated by stimulation of the proteins SOCS. SOCS can then inhibit cytokine signaling by binding to and inhibiting JAK/STAT.

Long Term Effects of Inflammatory Cytokines

The combined increased levels of IL-6 and IL-1β in an acute-phase response increases the risk of developing type II diabetes three-fold (Spranger et al., 2003). Studies have shown that chronically increased levels of IL-6 are associated with an increased risk of developing type II diabetes (Pickup and Crook, 1998). Both IL-6 and IL-1β act on the liver to produce characteristics of metabolic syndrome such as insulin resistance (Pickup

and Crook, 1998), and skeletal muscle which causes atrophy during states of chronic stress (Späte and Schulze, 2004). In addition, studies have shown increased levels of amniotic (Kupferminc et al., 1994) inflammatory cytokines in cases of IUGR (Heinig et al., 2000; Holcberg et al., 2001; Alisi et al., 2011). Elevated concentrations of inflammatory cytokines in amniotic fluid have been linked to irregular immune activation, leading to the pathophysiology of IUGR (Bartha et al., 2003). Studies suggest that administration of bacterial lipopolysaccharide (LPS) endotoxin to induce maternal inflammation in the second half of pregnancy reduced fetal weight significantly in rats when compared to control dams treated with saline (Cadaret et al., 2017a), suggesting that systemic maternal inflammation is impacting fetal weight by causing fetal inflammation. In conclusion, maternal inflammation correlates with a decrease in placental growth, particularly reduced thickness, and a decrease in length and area, (Cotechini et al., 2014), which is known to cause smaller postnatal body size and development of metabolic deficiencies later in life (Barker et al., 2010). The chronic effects of pro-inflammatory cytokines are complex and are linked to the development of insulin resistance (Marette et al., 2014), which ultimately manifests in metabolic syndrome (Dandona et al., 2005).

Nonsteroidal Anti-Inflammatory Drugs and Pregnancy

Fetal exposure to inflammatory cytokines during gestation leads to metabolic adaptations that can be detrimental after birth and into adulthood such as insulin resistance and obesity (Pickup and Crook, 1998). NSAIDS (nonsteroidal anti-inflammatory drugs) are used to treat inflammatory responses by inhibiting cyclooxygenase (Østensen, 1996). Pregnant women are currently discouraged from

taking NSAIDS. The use of NSAIDS during pregnancy is thought to cause miscarriage (Li et al., 2003), intracranial hemorrhaging (Rumack et al., 1981), and renal failure (Cantor et al., 1980). However, there have been minimal studies conducted on fetal exposure to NSAIDS (van Gelder et al., 2011).

Elevated Steroid Concentrations and Gestation

Polycystic Ovary Syndrome

Polycystic ovary syndrome (PCOS) is an endocrine disorder that affects 5-10% of females of reproductive age (Franks, 1995). Females with PCOS experience ovarian cysts, irregular menstrual cycles, and hyperandrogenism. Furthermore, PCOS is accompanied by metabolic deficiencies such as insulin resistance and obesity (Faloia et al., 2004). Elevated androgen levels seen in females with PCOS remain even during pregnancy (Sir-Petermann et al., 2002). Androgens including testosterone can reduce fetal and newborn growth in offspring from females with hyperandrogensim (Carlsen et al., 2006).

Effects of Elevated Androgen Levels on Fetal and Newborn Growth

Exposure to excess androgens during critical periods of gestation can lead to reduced birth weight (Carlsen et al., 2006) and metabolic deficiencies in offspring (Smith et al., 2009). Female fetuses exposed to elevated testosterone during gestation have impaired insulin secretion and increased adiposity later in life (Eisner et al., 2000). In ewes, prenatal exposure to elevated testosterone levels causes IUGR (Steckler et al., 2005). Recent studies indicate that exposure to androgens during fetal development

induces metabolic deficits which may be due to programming of metabolic pathways (Abbott et al., 2005).

Conclusion

It is well known that maternal stress has adverse effects on the development of a fetus's muscle growth and metabolic function leading to the development of metabolic syndrome later in life. Evidence suggests that maternal inflammation is causing fetal inflammation either directly or indirectly by causing placental insufficiency. Pregnant women are currently discouraged from taking NSAIDS because it has been shown to cause unfavorable neonatal outcomes (Cantor et al., 1980; Rumack et al., 1981; Li et al., 2003). However, the aim of current research is to understand whether chronic inflammation during pregnancy is more damaging to the fetus than the effects of NSAIDS that treat chronic inflammation. By understanding the underlying mechanism causing fetal inflammation, we will be able to better address the pathophysiology and prevention of long-term metabolic diseases in humans and livestock, improving quality of life. More specifically directed towards livestock production, increased meat quality and profit for the producer can be achieved.

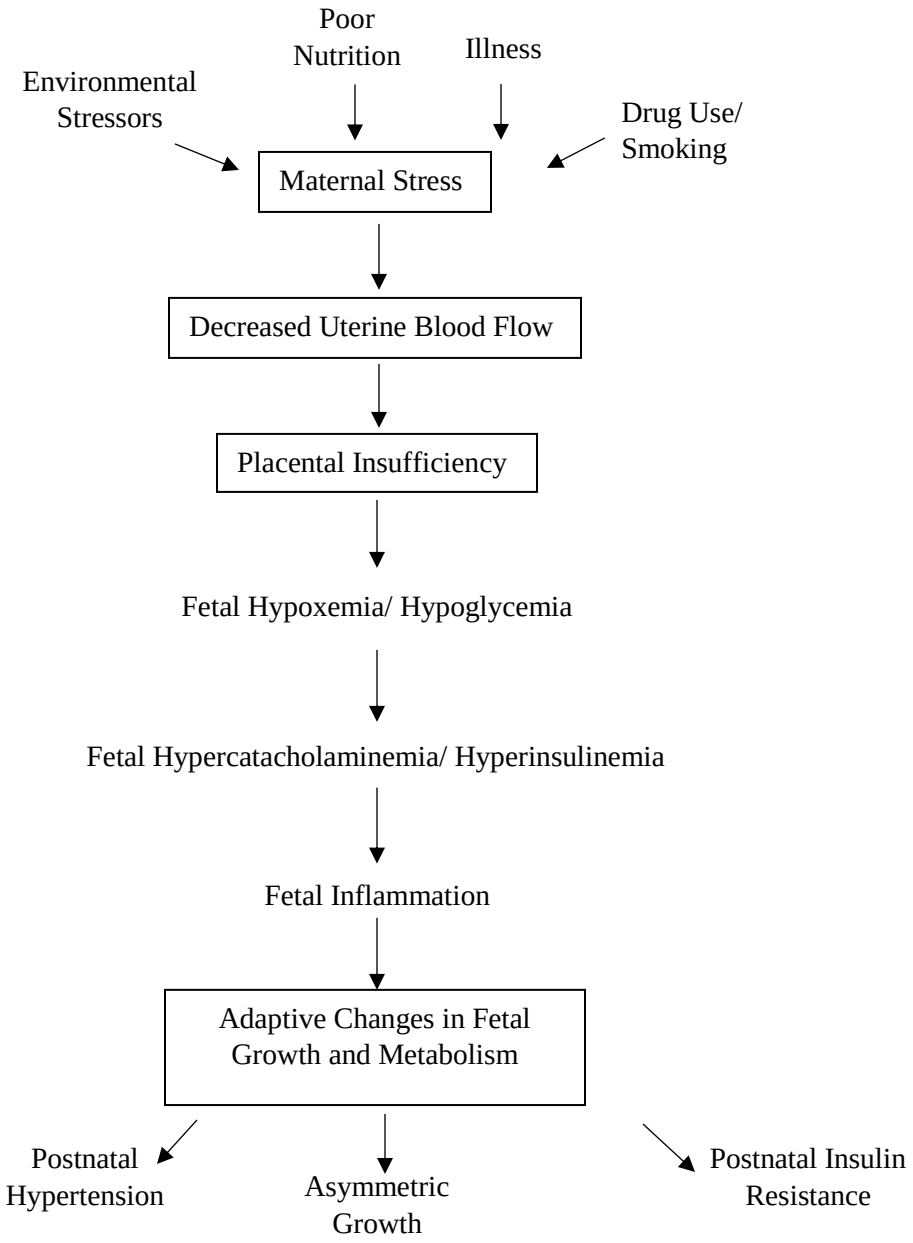

Figure 1. Maternal stressors lead to adaptive fetal changes in growth and metabolism by stunting the placenta. Placental insufficiency ultimately leads to fetal inflammation by causing hypoxemia, hypoglycemia, hypercatacholaminemia, and hyperinsulinemia. The perinatal effects of these factors include hypertension, asymmetric growth, and insulin resistance.

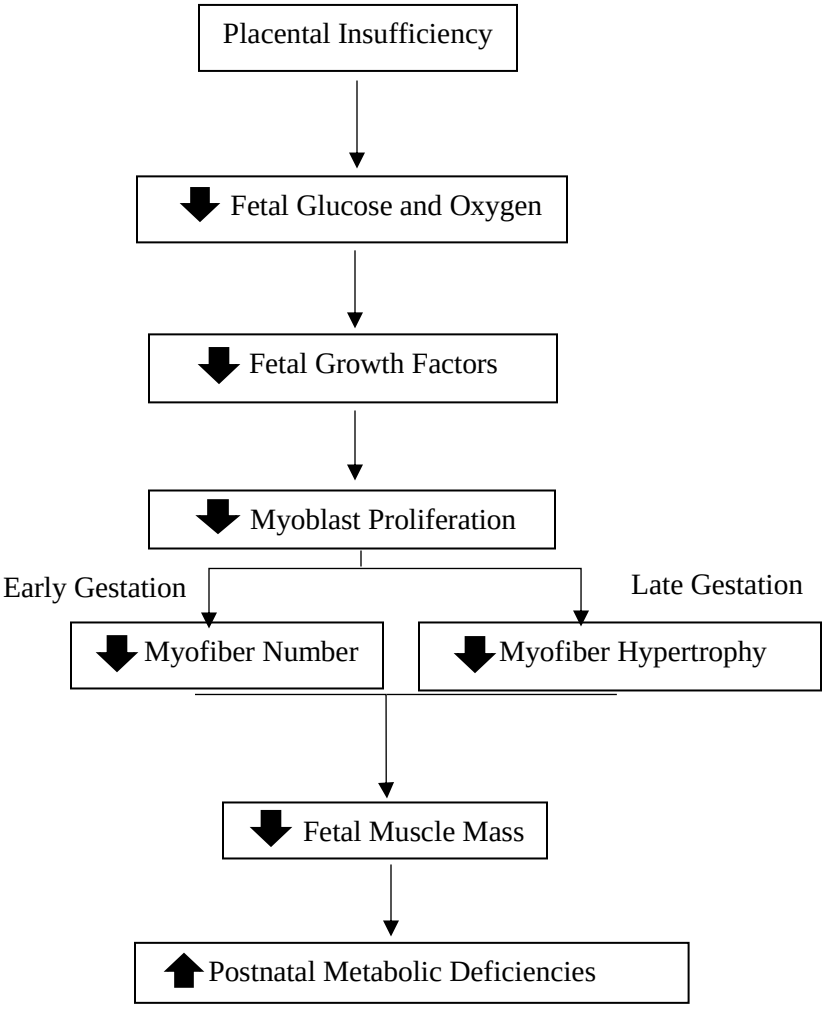

Figure 2. During conditions of placental insufficiency, fetal muscle mass is greatly impacted. A reduction in fetal muscle mass will ultimately lead to an increased risk of developing metabolic deficiencies later in life due to skeletal muscle being a primary tissue for glucose utilization.

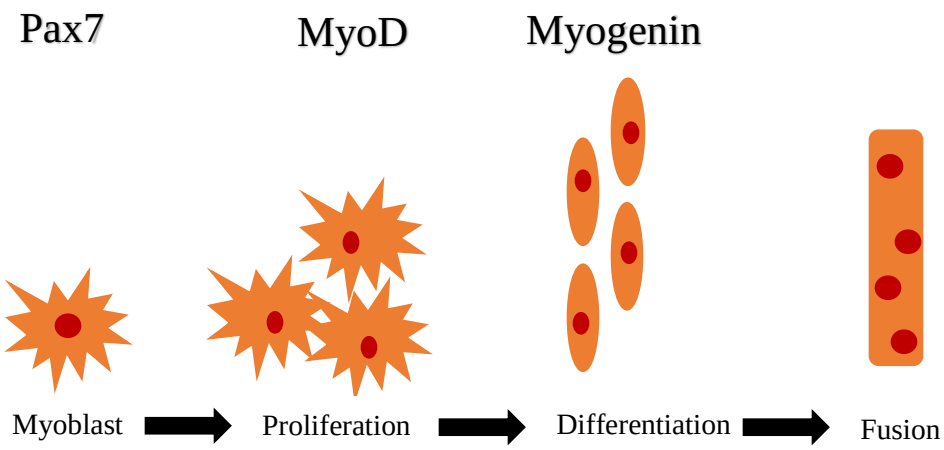

Figure 3. Activated myoblasts will proliferate, differentiate, and fuse and with myofibers. Each of these stages is characterized by expression of specific muscle regulatory factors (MRF) transcription factors.

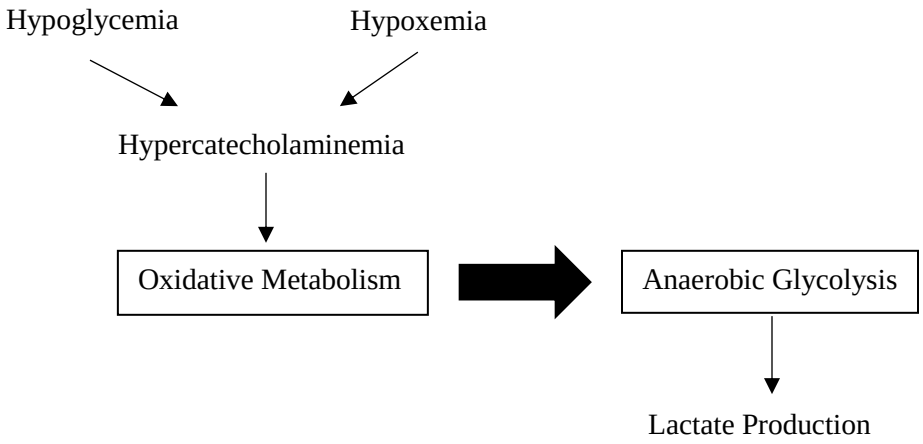

Figure 4. Hypercatecholaminemia and hypoxemia experienced during fetal stress causes a metabolic shift from aerobic glycolysis to anaerobic glycolysis, leading to excess lactate production.

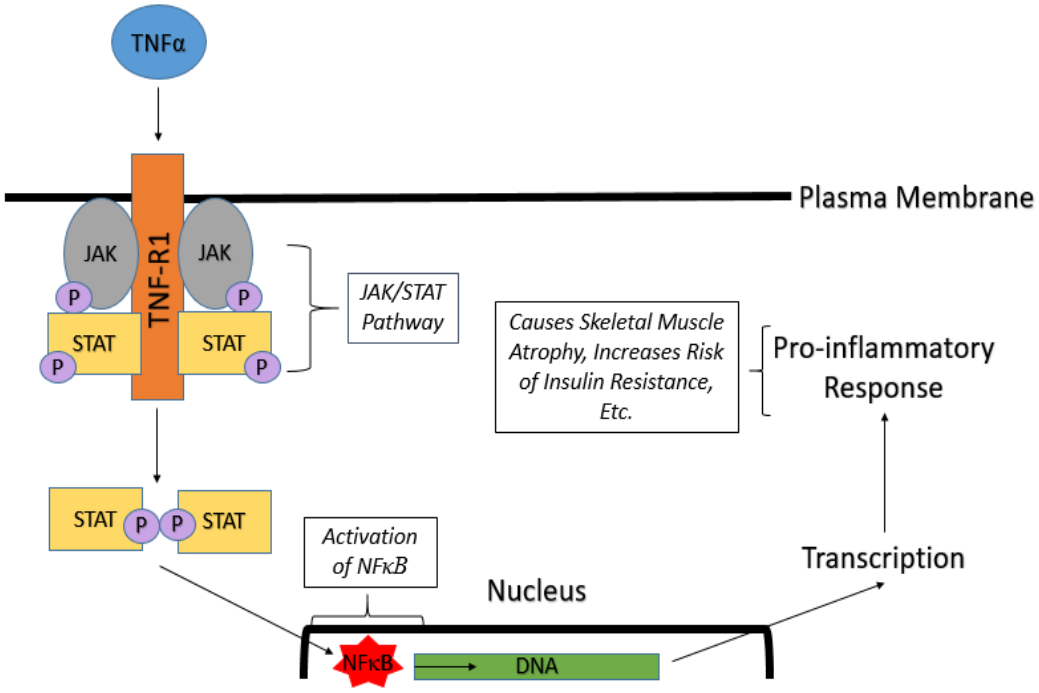

Figure 5. Inflammatory cytokine signal transduction pathway.

Chapter 2

Maternal inflammation in the pregnant ewe at 0.7 gestation impairs glucose oxidation in fetal skeletal muscle near term

Abstract. Placental insufficiency caused by maternal stress during gestation is known to decrease birth weight and increase the risk of offspring developing metabolic deficiencies such as insulin resistance and obesity. However, the underlying mechanisms remain to be understood. Our objective was to determine if chronic maternal stress impairs subsequent glucose metabolism rates in fetal sheep near term. Pregnant ewes were treated with saline (controls) or bacterial endotoxin (LPS) every 3rd day from day 100-115 of gestation (term = 150 days) to induce systemic inflammation. On gestational day 125, ewes were euthanized and fetal soleus muscle was isolated tendon-to-tendon and split longitudinally. To determine glucose uptake and glucose oxidation rates, soleus strips were incubated in KHB (Krebs Henseleit Buffer) that was un-spiked (basal) or spiked with either insulin or TNFα. In addition, Akt phosphorylation in extensor digitorum longus muscle samples was determined by western immunoblot analysis and Myosin heavy chain (MyHC) content was determined using electrophoresis. Furthermore, fiber type numbers and sizes were determined from fetal semitendinosus sections by immunohistochemistry. In primary fetal soleus muscle, glucose uptake was not different between control and maternal inflammation fetuses under basal, insulin-stimulated, or TNFα-stimulated conditions. However, insulin-stimulated glucose oxidation and TNFα-stimulated glucose oxidation were both greatly decreased ($P < 0.05$) in chronically stressed fetal muscle compared to controls. In addition, Akt phosphorylation was decreased ($P < 0.05$) after maternal inflammation when compared to controls. However, there were not differences

in MyHC content or skeletal muscle fiber number but Type IIx muscle fiber area was decreased ($P < 0.05$) after maternal inflammation when compared to controls. Our findings indicate that glucose metabolism in fetuses is impaired after chronic maternal inflammation which explains in part how stress-induced IUGR caused by maternal stressors increases the risk of insulin resistance in offspring. Phosphorylation of Akt in insulin cultures is diminished which indicates that decreased Akt phosphorylation is the mechanism causing impaired glucose metabolism rather than differences in skeletal muscle fiber proportions.

Introduction

Infants born small for gestational age as a result of IUGR are known to be at an 18-fold greater risk for developing metabolic syndrome later in life (Gatford et al., 2010). Reduction in muscle mass contributes to reduced size at birth, as less muscle is advantageous for fetuses developing in a harsh uterine environment because limited nutrients can be redirected to more vital brain and heart tissues (Hales and Barker, 2001). Skeletal muscle accounts for greater than 80% of insulin-stimulated glucose metabolism (DeFronzo et al., 1981) and therefore plays a major role in glucose homeostasis (Yates et al., 2012).

Insulin is known to increase glucose uptake in skeletal muscle by binding to its tyrosine kinase receptor and activating a signaling cascade that ends with the GLUT4 transporter being translocated to the cell membrane, where it facilitates glucose transport into the cell. Akt phosphorylation is a critical step in the insulin signaling pathway that contributes to many of insulin's effects on the cell (James et al., 1988). In this study, we

determined whether changes in glucose metabolism coincide with changes in Akt phosphorylation rates, which could help explain reduced insulin sensitivity.

Inflammatory cytokines such as TNFα and IL-6 acutely stimulate skeletal muscle glucose oxidation similarly to insulin, despite disrupting insulin signaling (Cadaret et al., 2017b). However, chronic exposure to inflammation may reduce sensitivity to cytokines. We hypothesize that fetal muscle that has been chronically inflamed due to maternal inflammation during the third trimester of pregnancy will become less responsive to the stimulatory effects of inflammatory cytokines, which can ultimately lead to the development of insulin resistance (Pickup and Crook, 1998; Spranger et al., 2003). We speculate that stressed fetuses with reduced muscle mass will have a decrease in glucose uptake and oxidation when compared to controls.

Materials and Methods

Animals. The following experiments were approved by the Institutional Animal Care and Use Committee at the University of Nebraska-Lincoln. Studies were conducted at the University of Nebraska-Lincoln Animal Science Complex which is accredited by the American Association for Accreditation of Laboratory Animal Care. Animals used for this study included thirteen timed-bred Polypay ewes carrying ultrasound-verified twin pregnancies. Polypay ewes carrying twins received an IV injection of sterile saline (Controls; n = 8) or 0.1 μg/kg BW of bacterial lipopolysaccharide (LPS; n = 5) from *E. coli O55:B5 (*Sigma-Aldrich, St. Louis, MO*)* every third day from day 100 to 115 of gestation (term = 150 days) (Figure 1).

Glucose Uptake. Soleus muscle (100-500 mg) was utilized for this experiment due to its increased type I muscle fiber ratio, thus having high oxidative capacity. The muscle was isolated tendon to tendon during necropsy from fetal sheep at 125 dGA. Pre-incubation, wash, and incubation media were spiked with the following treatments: none (basal), insulin (5 mU/ml Humulin-R), or TNFα (20 ng/ml hTNFα). All additives were purchased from Sigma-Aldrich (St. Louis, MO). Muscle strips were incubated at 37º C for 20 minutes in treatment spiked KHB with 1 mM [^{3}H]2-deoxyglucose and 39 mM [^{14}C] mannitol. Muscle strips were removed and washed thrice in ice-cold PBS, weighed, and lysed in 2 M NaOH at 37º C for 1 hour. Lysate was mixed with scintillation fluid and specific activity of [^{3}H] and [^{14}C] was measured. Specific activity of media was also determined.

Glucose Oxidation. Muscle strips were placed in sealed dual-well chambers and incubated at 37º C for 2 hours in treatment-spiked KHB with 5 mM [^{14}C-U] D-glucose. 2 M NaOH was put into the adjacent wells to collect $^{14}CO_2$. After the 2 hour incubation, the chambers were cooled at -20º C for 2 minutes. 2M HCl was injected into the media through the rubber seal. Chambers were placed at 4º C for 1 hour. Chambers were opened and muscle strips were washed and weighed. The NaOH was collected and mixed with scintillation fluid to determine the specific activity of $^{14}CO_2$. Specific activity of media was also measured.

Myosin heavy chain electrophoresis. Fetal extensor digitorum longus muscle (100-500 mg) was used due to its high oxidative capacity. The muscle was split longitudinally and muscle strips were incubated in insulin-spiked KHB for 20 minutes, snap frozen, and stored at -80ºC. The muscle strips were homogenized in 200 µl of RIPA

buffer containing manufacturer recommended concentrations of Halt Protease and Halt Phosphatase Inhibitor Cocktails (Thermo Fisher). Homoginates were sonicated and centrifuged (2,500 x *g*; 10 minutes). Supernatant was collected and total protein concentrations were determined by Pierce BCA Assay (Thermo Fisher). Samples were then incubated at room temperature for 10 minutes., heated at 70ºC for 10 minutes., combined with Bio-Rad 4X Laemmli Sample Buffer (Bio-Rad, Hercules, CA) to a 1X concentration, and loaded onto a separating gel at 15 µg/well. Myosin heavy chain isoforms were then separated by SDS-Page. The separating gel consisted of 35% glycerol, 9% acrylamide/bisacrylamide (50:1), 230mM Tris (pH 8.8), 115mM glycine, 0.4% SDS, 0.5% TEMED, and 0.1% APS. The gel was poured between plates, overlaid with water, and allowed to polymerize for 10 minutes. After polymerization, water was removed using blot paper. Stacking gel consisted of 47% glycerol, 6% acrylamide/bisacrylamide (50:1), 110mM Tris (pH 6.7), 6mM EDTA, 0.4% TEMED, and 0.1% APS. This gel was poured on top of the polymerized separating gel. The comb was inserted and gel was allowed to polymerize for 15 minutes. Protein samples were prepared by combining 15 µg of protein with 4X sample buffer (to 1X). Samples were incubated at room temperature for 10 minutes then put on a dry bath at 70ºC for 10 minutes. To run the SDS-page, the comb was removed and wells were rinsed with water, wells were loaded at 15 µg/well, and gel was run at 100 volts for 30 hours at 4ºC. After electrophoresis, the SDS-Page was washed and stained with GelCode Blue Stain Reagent overnight. Samples were then imaged using an Odyssey infrared imaging system (LI-COR Biosciences, Lincoln, NE). Myosin heavy chain I and myosin heavy chain II bands

were measured by densitometry (Image Studio Lite Ver 5.0; LI-COR) and normalized to total MyHC protein content.

Western Immunoblot. The activation of Akt was estimated by the proportions of phosphorylated to total Akt protein as previously described (Cadaret et al., 2017b), with minor modifications. Phosphorylated Akt and total Akt protein concentrations were determined in fetal extensor digitorum longus muscle strips that were incubated in insulin-spiked KHB for 20 minutes, snap frozen, and stored at -80ºC. Muscle strips (100-500 mg) were homogenized in 200 µl of radioimmunoprecipitation buffer containing manufacturer-recommended concentrations of Protease and Phosphate Inhibitor (Thermo Fisher, Carlsbad, CA). Homogenates were sonicated and centrifuged (14,000g for 5 minutes at 4ºC), then supernatant was collected. Total protein concentrations were determined by Pierce BCA Protein Assay Kit (Thermo Fisher). Protein samples were boiled for 5 minutes. at 95ºC in BioRad 4X Laemmli Sample Buffer (BioRad, Hercules, CA) then separated by SDS-polyacrylamide. Protein samples were diluted into 4X sample buffer (to 1X) and incubated at room temperature for 10 minutes. Samples were then put in a dry path at 70ºC for 10 minutes. Protein was loaded for electrophoresis and gel was run at 100 volts for 30 minutes at 4ºC. Gels were transferred to polyvinylidene fluoride low florescence membranes (BioRad) which had been incubated in Odyssey block solution (Li-Cor Biosciences, Lincoln, NE) for 1 hour at room temperature and washed with 1X TBS-T (20mM Tris-HCl + 150mM NaCl + 0.1% Tween 20). Membranes were then incubated with one of the following rabbit antibodies diluted in Odyssey block solution + 0.05% Tween-20: anti-phospho-Akt (Cell Signaling, Danvers, MA) (1:2000) for 1 hour at room temperature or anti-Akt (9272) (1:1000) at 4ºC

overnight. An IR800 goat *anti*-rabbit IgG secondary antibody (1:10,000) diluted in Odyssey block solution with 0.05% Tween-20 and 0.01% SDS was applied for 1 hour at room temperature. Blots were scanned on an Odyssey Infrared Imaging System and analyzed with Image Studio Lite Software (Li-Cor). For each protein of interest, phosphorylation rates were estimated by the proportions of phosphorylated protein to total protein.

Immunohistochemistry. Isolated semitendinosus muscle was fixed in 4% PFA for 48 hours, 30% sucrose for 24 hours, and 50:50 OCT: 50% sucrose mixture for 24 hours. A cross section of muscle was embedded in OCT (Fisher HealthCare, Houston, TX) and stored at -80ºC. Muscle tissue was then sectioned by cryostat and mounted on glass microscope slides at 8µm, two cross sections per slide, and stored at -80ºC. Before staining, slides were dried in an Isotemp Oven (Thermo Scientific, Waltham, MA) at 37ºC for 30 minutes. and rehydrated in PBS+ (PBS with 0.5% Triton-X-100) 3 x 5 minutes each. Slides were fully submerged in citric acid (10mM) and microwaved at 40% power 4 x 5 minutes each and cooled for about 1 hour and submerged in PBS+ 3 x 5 minutes each. 50µl of NEN blocking agent (0.5% NEN) was used to cover each cross section and each tissue was overlaid with Parafilm (Bemis, Neenah, WI) and incubated for 1 hour at room temperature in a humidified container. One of the following primary antibodies diluted in PBS + 1% BSA were added to tissue sections to detect myosin heavy chain I or IIx: 0.2 µg/ml BA-D5 or 2 µg/ml 6H1, respectively Each tissue was also co-stained for Desmin (1:300, Sigma). Slides were incubated overnight at 4ºC in a humidified container. On the second day, slides were washed in PBS+ 3 x 5 minutes. each. One of the following secondary antibodies diluted in PBS + 1% BSA were added to

tissue sections to detect myosin heavy chain I or IIx: 1:2000 Alexa Fluor 594 IgG or 1:2000 594 IgM (Cell Signaling, Danvers, MA), respectively. Slides were incubated for 2 hours at room temperature in a humidified container. Slides were washed for 5 minutes in PBS+ then submerged in double distilled H_2O 2 times for 5 minutes each. 100µl per slide of DAPI (1:1000 in double distilled H_2O) (Sigma) was added and slides were incubated at room temperature for 4 minutes. Slides were washed in double distilled H_2O for 5 minutes and then 250 µl of 0.3% Sudan Black (Fisher Scientific, Waltham, MA) was added to each slide for 20 minutes at room temperature in a humidified container. Slides were washed in double distilled H_2O 3 x 5 minutes each. Slides were then coverslipped with 100µl of Tris buffered mounting media (0.1M). Staining was visualized using Olympus CellSense Software to determine proportions and average cross-sectional areas of positively-stained fibers within muscle sections.

Statistical Analysis. Data were analyzed by ANOVA using the GLM procedure of SAS (SAS Institute, Cary, NC). Glucose uptake and glucose oxidation data were analyzed as two different experiments, each with its own basal, insulin, and TNFα conditions. Two separate muscle strip from each fetus was exposed to each condition in the experiment and averaged. Fetus was the experimental unit (control, n=8, maternal inflammation, n=6). Glucose metabolic rates are normalized to muscle strip mass and presented as percentage change from basal conditions. Data are presented and means ± standard error.

Results

Glucose Uptake. Incubation with insulin increased ($P < 0.05$) glucose uptake in fetal soleus muscle from both control and after maternal inflammation by ~30% and

~26%, respectively (Figure 2). Moreover, glucose uptake rates in fetal muscle strips incubated with TNFα was increased ($P < 0.05$) in both control and after maternal inflammation by ~48% and ~28% from basal conditions, respectively, and was not different from muscle incubated with insulin for either treatment group.

Glucose Oxidation. An interaction ($P < 0.05$) was observed between maternal treatment and incubation media for glucose oxidation (Figure 3). Incubation in media spiked with insulin increased ($P < 0.05$) glucose oxidation in fetal muscle from both treatment groups, but the increase was greater ($P < 0.05$) in fetal muscle from control fetuses than after maternal inflammation by ~19%. Moreover, when muscle from control fetuses was incubated with TNFα, glucose oxidation was ~69% greater ($P < 0.05$) than when incubated under basal conditions but less by ~12% ($P < 0.05$) than when incubated with insulin. Conversely, when muscle from fetuses after maternal inflammation was incubated with TNFα, glucose oxidation rates did not increase above basal conditions.

Akt Phosphorylation. Insulin stimulated phosphorylation of Akt was decreased ($P < 0.05$) in the fetal muscle strips after maternal inflammation compared to controls and was not different from muscle incubated under basal conditions (Figure 4). Furthermore, there was no difference in Akt phosphorylation between fetal muscle strips from either treatment stimulated with TNFα compared to basal.

Myosin Heavy Chain Expression. Proportions of Type I fibers and Type IIx fibers were identified by MyHC staining (Figure 5). There were no differences in fiber type numbers between fetal semitendinosus from control fetuses and after maternal inflammation for Type I or Type IIx fibers (Figure 6). Furthermore, there was a decrease ($P < 0.05$) in Type IIx fiber area by ~57% after maternal inflammation compared to

control fetuses (Figure 7). In addition, there was no difference in myosin heavy chain ratios between control and chronically stressed fetuses (Figure 8).

Discussion

In this study, we show that insulin responsiveness of glucose oxidation is impaired in fetal skeletal muscle after chronic maternal inflammation. This helps to explain how IUGR born individuals are at an increased risk of developing metabolic diseases, despite the fact that capacity for insulin-stimulated glucose uptake in fetal muscle was not affected by chronic maternal inflammation. Moreover, stimulation of glucose oxidation by inflammatory cytokines was diminished by fetal adaptations to chronic maternal inflammation, even after inflammation had been alleviated. Additionally, insulin-stimulated Akt activation was impaired in fetal skeletal muscle after chronic maternal inflammation, which shows that disruptions in insulin signaling are contributing to impaired glucose oxidation. Furthermore, we determined that reduced glucose oxidative capacity was not attributable to changes in fiber type proportions as these were not different between treatment groups. Interestingly, maternal inflammation did lead to smaller Type IIx fibers but not Type I fibers. These findings may help to explain previous findings showing that chronic inflammation during fetal development increases the risk of developing insulin resistance later in life (Hotamisligil et al., 1993).

This study also shows exposure of fetal skeletal muscle to chronic inflammation inhibits TNFα-stimulated glucose oxidation, which was observed in controls. Our previous studies show that acute exposure to inflammatory cytokines increases glucose oxidation in muscle even in the absence of insulin (Cadaret et al., 2017b). However, the present study shows that chronic exposure to inflammation during fetal development

decreases this metabolic response and that subsequent stimulation by cytokines does not produce greater glucose oxidation. Thus, the acute benefit of this metabolic regulator is lost even though other changes associated with cytokines such as insulin insensitivity likely still occur.

Skeletal muscle fiber type ratios were not affected by chronic maternal inflammation. While fiber type number was not different between treatments, the area of Type IIx fibers was decreased after maternal inflammation compared to controls. This indicates that there is no difference in the inherent oxidative capacity between skeletal muscle of the two groups of fetuses per se, but rather a reduced capacity to respond to insulin. Insulin-stimulated fetal skeletal muscle showed a reduction in activation of Akt after maternal inflammation. This shows that the impaired response to insulin is associated with chronic stress at least in part due to inflammatory adaptations. Thus, impairment of downstream hubs such as Akt may be major contributors to the decrease in glucose oxidation in chronically stressed fetuses rather than diminished proportions of Type I oxidative fibers.

In conclusion, our study shows that fetuses exposed to chronic maternal inflammation develop decreased insulin-stimulated glucose oxidation rates despite normal oxidative capacity as indicated by fiber type proportions. Rather, Akt activation by insulin is substantially decreased by chronic maternal inflammation. This suggests that the decreased oxidation rate stems from adaptive impairment in insulin signaling.

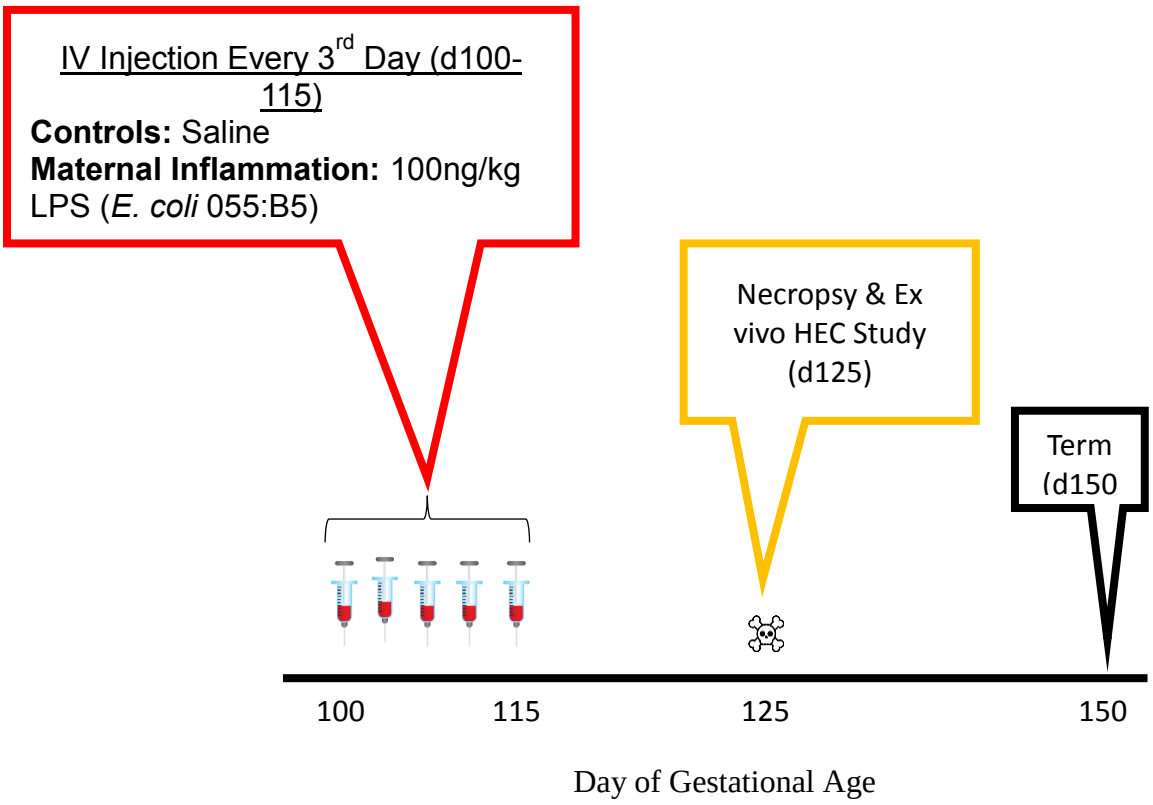

Figure 1. Polypay ewes carrying twins received an IV injection of sterile saline (Controls; n = 8) or 0.1 µg/kg BW of bacterial lipopolysaccharide (LPS; n = 5) every third day from day 100 to 115 of gestation.

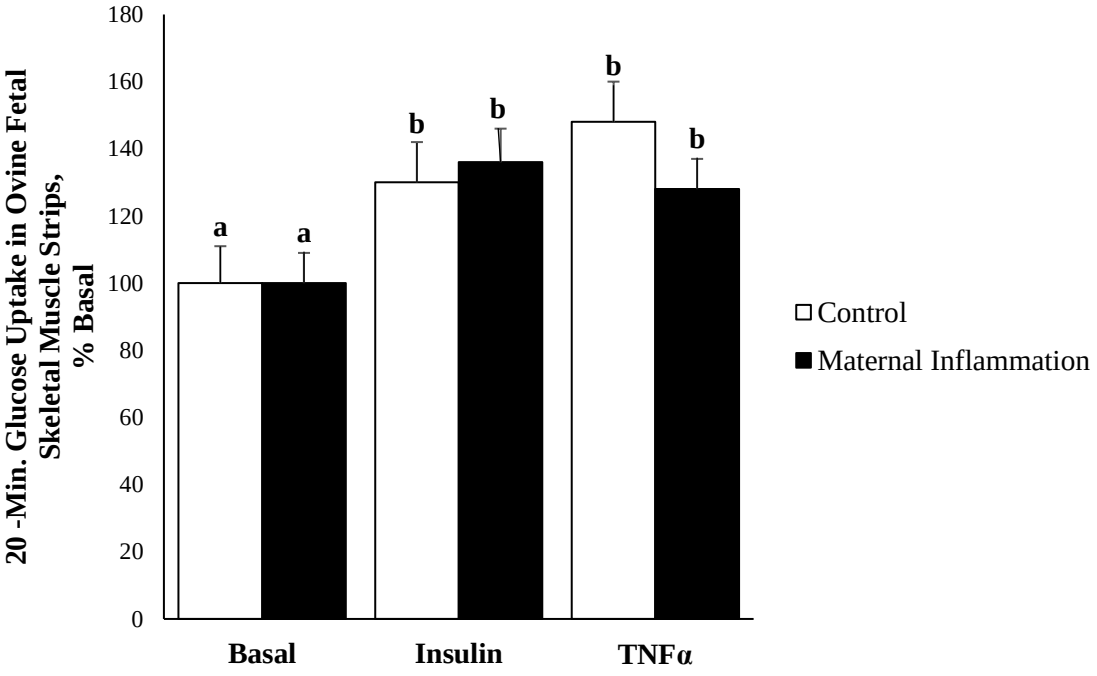

Figure 2. Glucose uptake in fetal soleus muscle strips after maternal inflammation during 20 minute incubations spiked with one of the following treatments: No additive (basal), Insulin (5mU/ml Humulin-R), or TNFα (20ng/ml hTNFα), respectively. ^{a,b} means with differing subscripts differ ($P<0.05$).

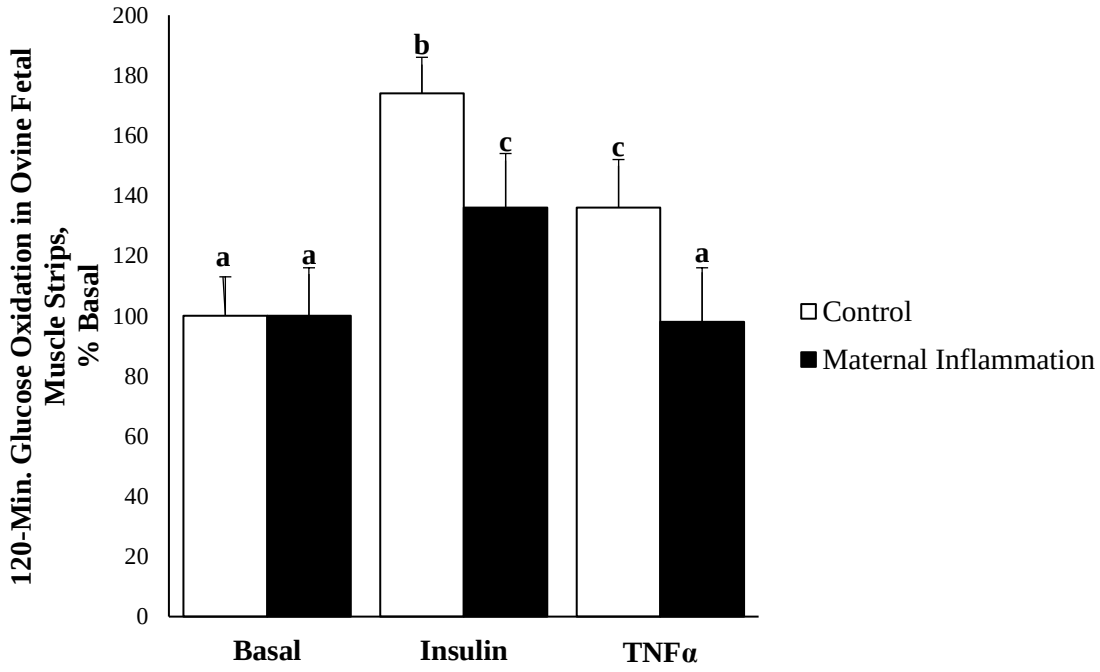

Figure 3. Glucose oxidation in fetal soleus muscle strips after maternal inflammation during 120 minute incubations spiked with one of the following treatments: No additive (basal), Insulin (5mU/ml Humulin-R), or TNFα (20ng/ml hTNFα), respectively. ^{a,b,c} means with differing subscripts differ ($P<0.05$).

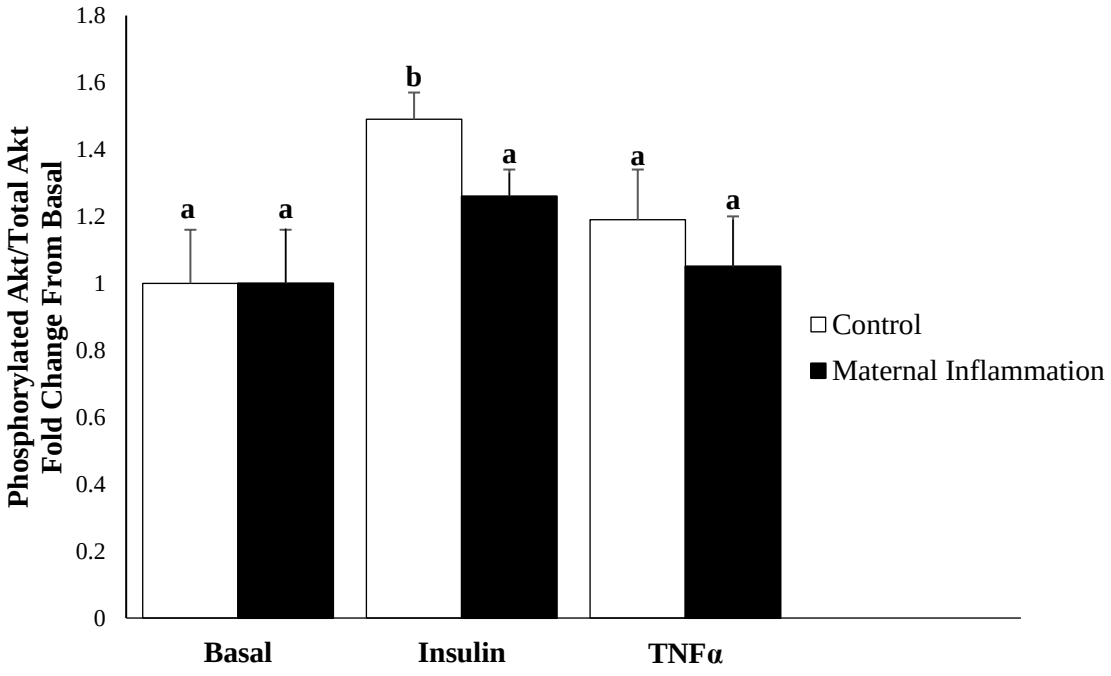

Figure 4. Akt phosphorylation in fetal extensor digitorum longus muscle after chronic maternal inflammation stimulated by one of the following treatments: No additive (basal), insulin (5mU/ml Humulin-R), or TNFα (20ng/ml hTNFα), respectively. ^{a,b} means with differing subscripts differ (P<0.05).

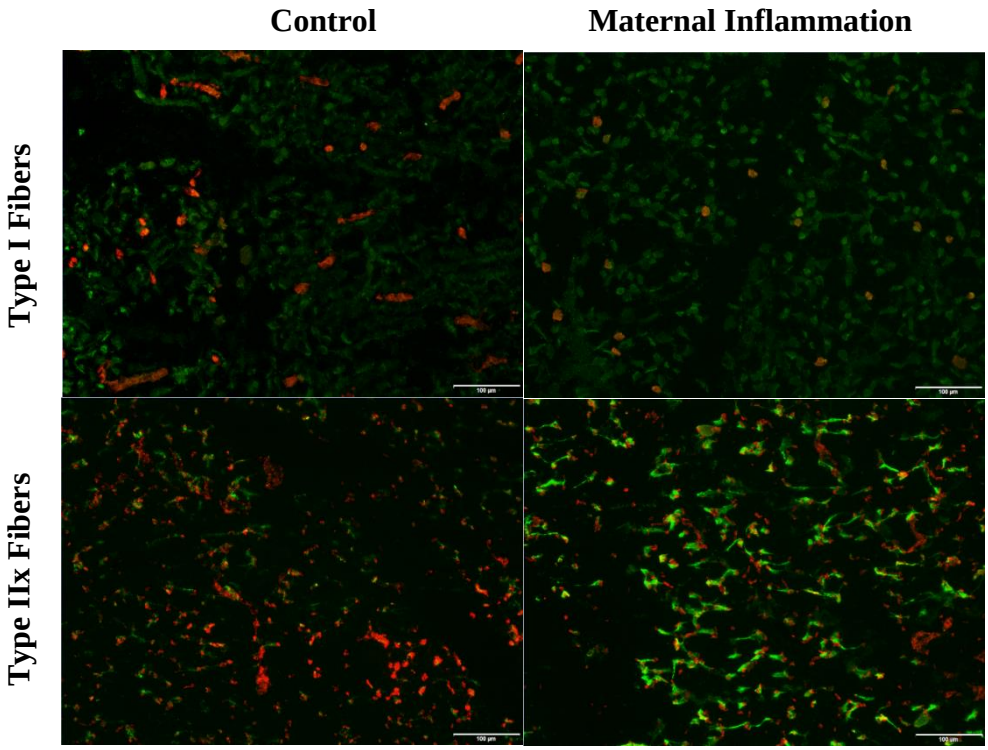

Figure 5. Immunostaining for fiber type in fetal semitendinosus muscle. Representative micrographs are depicted for control and after maternal inflammation semitendinosus cross sections (8 μm). Sections were stained for myosin heavy chain isoforms (red) and counterstained for desmin (green). Bar = 100 μm.

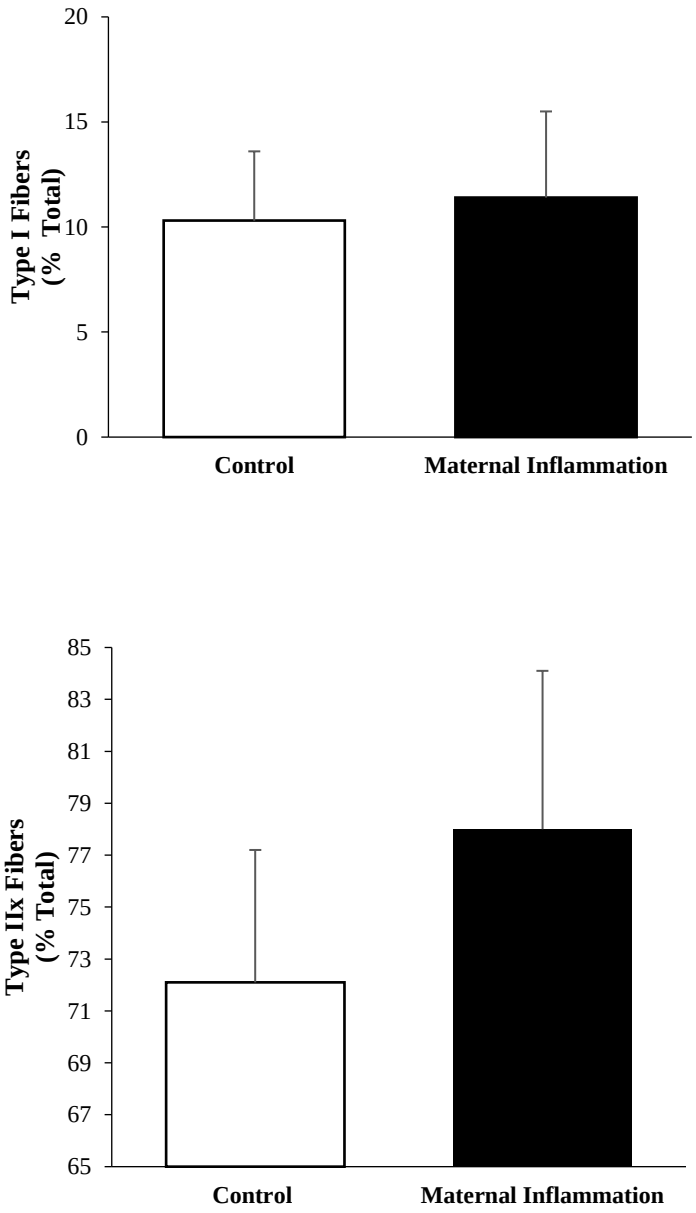

Figure 6. Muscle fiber-type proportions. The percentages of total fibers are presented for control and chronically stressed fetal semitendinosus muscle sections. Type I and Type IIx fibers were determined by immunohistochemistry. All sections were counterstained for desmin to determine total fiber numbers.

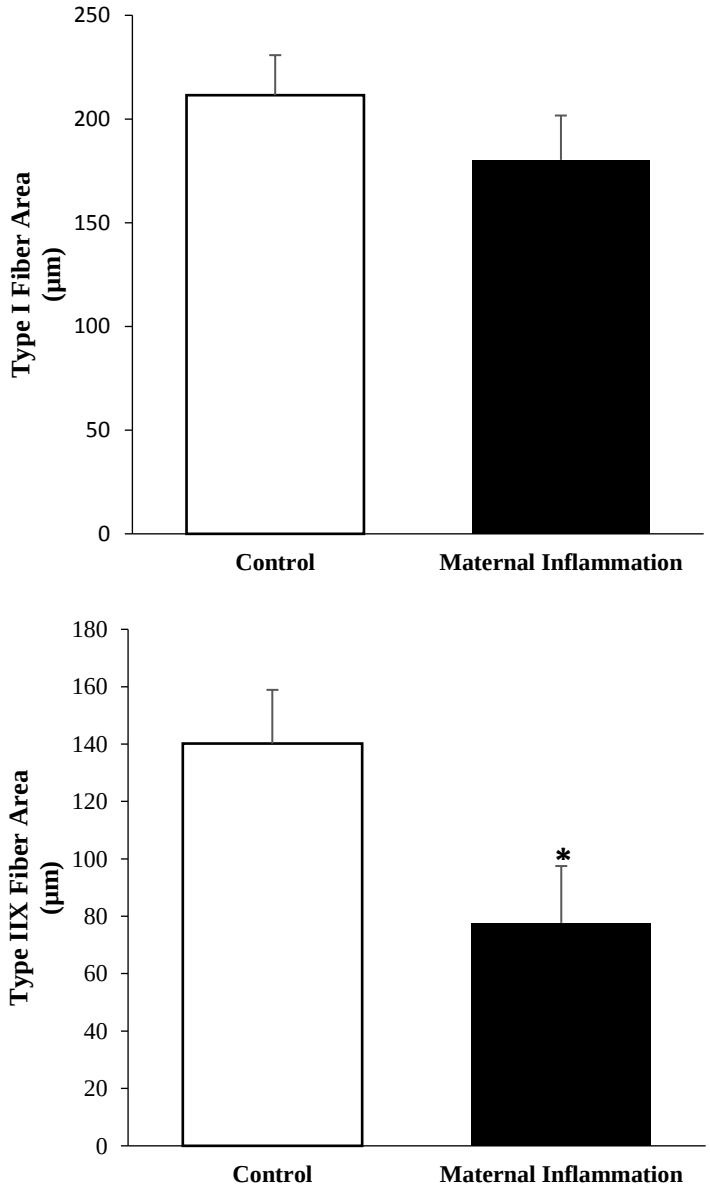

Figure 7. Muscle fiber cross-sectional areas presented for control and chronically stressed fetal semitendinosus muscle sections. Type I and Type IIx fibers were determined by immunohistochemistry. All sections were counterstained for desmin to determine total fiber numbers. *Means differ ($P < 0.05$) between treatment groups.

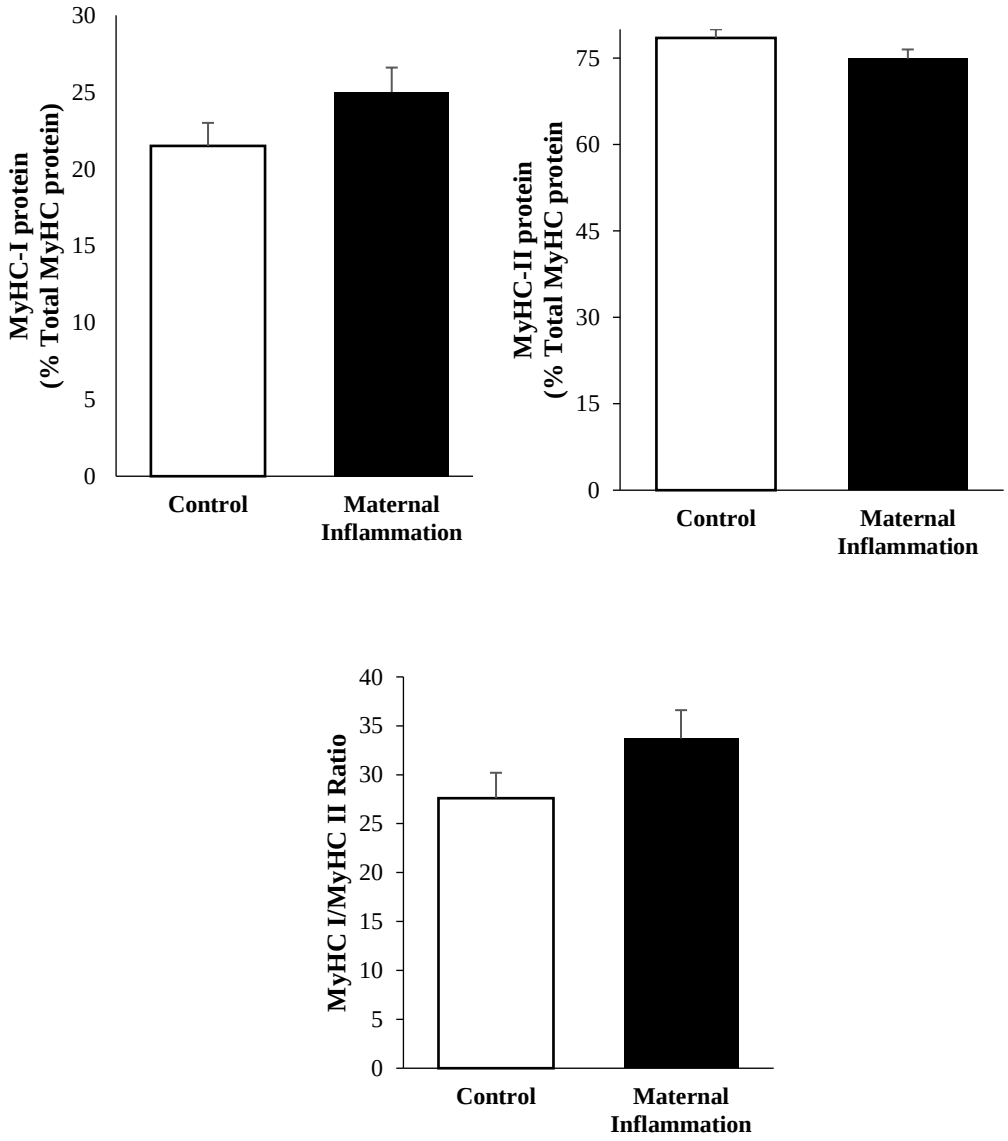

Figure 8. Myosin heavy chain protein content and ratio of myosin heavy chain I to myosin heavy chain II after chronic maternal inflammation. Electrophoretic mobility was used to separate MyHC-I and MyHC II fractions of total protein isolated from fetal extensor digitorum longus muscle.

Chapter 3

Metabolic response of bovine myoblasts exposed to sustained β adrenergic agonist stimulation during in vitro differentiation

Abstract. The β adrenergic agonists ractopamine HCl (β1) and zilpaterol HCl (β2) are commonly used as feed additives in finishing livestock to increase muscle deposition and decrease adipose accumulation, however the physiological mechanisms for these effects remain unclear. Previous studies conducted in our lab show that in adult rat skeletal muscle, acute stimulation with β2 agonist increases basal and insulin stimulated glucose oxidation in skeletal muscle from adult rats and growing lambs (Barnes et al., 2017; Cadaret et al., 2017b). Our objective was to determine the metabolic response of bovine myoblasts (muscle stem cells) differentiated in the presence of β adrenergic agonists in order to determine if the metabolic regulation by the β adrenergic system observed in skeletal muscle is contributed by muscle stem cells. Glucose uptake and glucose oxidation were determined in primary bovine myoblasts incubated for 4 days in differentiation media (2% FBS) with or without insulin, β1 adrenergic agonist, or β2 adrenergic agonist. Incubation with insulin alone increased ($P < 0.05$) glucose uptake by ~40% and oxidation by ~68% when compared to basal incubations. β2 adrenergic agonist alone likewise increased ($P < 0.05$) glucose uptake by ~54% and oxidation by ~49% from basal to levels that did not differ from insulin alone. β1 adrenergic agonist alone did not affect glucose uptake and only marginally increased ($P < 0.05$) glucose oxidation by ~18% from basal. Moreover, when β1 adrenergic agonist was combined with insulin, glucose uptake and oxidation were less ($P < 0.05$) than with insulin alone. Surprisingly,

when β2 adrenergic agonist was combined with insulin, glucose uptake was not different from insulin alone but glucose oxidation was decreased ($P < 0.05$) compared to insulin alone. Together, these findings show that β2 adrenergic agonists are more effective at increasing metabolic efficiency in myoblasts than β1 adrenergic agonists, just as in mature skeletal muscle. However, these findings also show that β2 adrenergic agonists do not have the same effect on insulin-stimulated glucose oxidation in myoblasts as they do in mature muscle, indicating that the entire metabolic phenotype of mature muscle is not derived from the muscle stem cells, and that key aspects of adrenergic regulation of glucose metabolism appear to develop within the fibers themselves.

Introduction

β adrenergic agonists, ractopamine HCl and zilpaterol HCl, sold under the trade names Optaflexx and Zilmax, respectively, enhance muscle growth and decrease fat accumulation in finishing cattle when used as feed additives (Mersmann, 1998). Pressure to increase feed efficiency due to a growing population, an increase in beef consumption, and competition for available land makes it beneficial for producers to use these products. This allows fewer resources and animals to yield more meat (Strydom, 2016) which benefits the U.S. agriculture economy (Centner et al., 2014). Zilpaterol HCl acts via β2 receptors and ractopamine HCl acts primarily via β1 receptors (Lean et al., 2014). We have recently shown that β2 adrenergic agonists enhance metabolic efficiency by increasing glucose oxidation in skeletal muscle (Cadaret et al., 2017b). However, it is important to know whether these effects originate within muscle stem cells that will ultimately fuse with skeletal muscle fibers or whether they originate within the mature fibers themselves. After birth, skeletal muscle grows by incorporating muscle stem cells

called myoblasts (Schultz, 1989; Allen and Rankin, 1990). Myoblasts increase the myonuclear content of skeletal muscle fibers after they are activated from their quiescent state to proliferate, differentiate, and fuse with existing muscle fibers (Allen and Boxhorn, 1989; Grounds and Yablonka-Reuveni, 1993). In fact, 50-99% of a muscle fiber's myonuclear content originates from myoblasts incorporated after the fiber is formed (Allen et al., 1979), thus myoblasts contribute greatly to the metabolic phenotype of the muscle. We recently found that skeletal muscle from mature rats and growing lambs exposed to β2 adrenergic agonist acutely and chronically, respectively, had increased insulin-stimulated glucose oxidation rates in culture (Barnes et al., 2017; Cadaret et al., 2017b). Since skeletal muscle development stems in large part from fusion of myoblasts, we hypothesize that this metabolic phenotype is inherited from the muscle stem cells via fusion with mature muscle fibers. Furthermore, differentiation of myoblasts in the presence of β agonists may also affect their responsiveness to β stimulation.

Materials and Methods

Animals. The following experiments were approved by the Institutional Animal Care and Use Committee at the University of Nebraska-Lincoln. Studies were conducted at the University of Nebraska-Lincoln Animal Science Complex which is accredited by the American Association for Accreditation of Laboratory Animal Care. Animals used for this study included four Angus-cross steers approximately one year of age that were humanely harvested at the UNL abattoir.

Myoblast Isolation. At harvest, 500g of fresh semitendinosus muscle was cleaned of all connective tissue and fat and finely minced. Minced muscle was placed in 50 ml conical tubes, washed with ice-cold phosphate buffered saline (PBS, Fisher Bioreagents),

and centrifuged at 1,500 x *g* for 5 minutes at 4ºC. Pelleted tissue was re-suspended in PBS, and digested with protease type XIV from *Strept. griseus* (Sigma) at a concentration of 625 mg/500 ml at 37ºC for 1 hour, and centrifuged at 1,500 x *g* for 5 minutes. Digested pellets were re-suspended in warm PBS and centrifuged at 500 x *g* for 10, 8, and 1 minute. After each spin, supernatant containing the myoblasts was collected, filtered, pelleted, and re-suspended in DMEM media. Cells were incubated in pre-plate media (DMEM with 10% FBS) at 37 ºC for 2 hours to remove fibroblasts. Myoblasts were collected, pelleted, re-suspended in freezing media (DMEM with 20% FBS and 10% dimethyl sulfoxide), slowly frozen, and stored in liquid nitrogen. All media constituents were purchased from Sigma-Aldrich except insulin, which was purchased from Eli Lilly.

Cell Culture. Bovine myoblasts were seeded onto 12-well fibronectin-coated tissue culture plates for glucose uptake studies and 6-well plates for glucose oxidation studies at an initial seeding density of 20,000 cells per well for both studies. Cells were grown as previously described (Yates et al., 2014) with some modifications. Briefly, all plates were coated with Poly-L-Lysine and Bovine Plasma Fibronectin. Cells were incubated in complete growth media (78.5% DMEM, 20% FBS, 1% Ab/Am, and 0.5% Gentamicin) for 24 hours then incubated in differentiation media (96.5% DMEM, 2% FBS, 1% Ab/Am, and 0.5% Gentamicin) for four days. Differentiation media was spiked with one of the following treatments: no additive (basal), insulin (5 mU/ml HumulinR), β1 agonist (1 μM ractopamine HCl), β2 agonist (0.05 μM zilpaterol HCl), β1 agonist + insulin, or β2 agonist + insulin (Figure 1). Differentiation media was changed every other day. After four days, glucose uptake and oxidation studies were performed.

Glucose Uptake. Cells were pre-incubated at 37ºC for 1 hour in treatment spiked Krebs-Henseleit Buffer (KHB) media containing 0.1% BSA, 5mM glucose, and 35 mM mannitol and then washed at 37ºC for 20 minutes in treatment-spiked glucose-free KHB media with 0.1% BSA and 40 mM mannitol. Finally, cells were incubated at 37º C for 20 minutes in treatment-spiked KHB media with 1 mM [^{3}H] 2-deoxyglucose (3,000 µCi/mmol) and 39 mM [U-^{14}C] mannitol (12.5 µCi/mmol), and 0.1% BSA. Media was then removed and cells were thrice washed with sterile saline. Cultures were fixed with 4% PFA (Sigma-Aldrich) for 20 minutes. then washed with sterile saline. Cells were nuclear stained with 5 µg/ml Hoeshst 3342 (Thermo-Fischer) diluted in sterile saline (Vet One, Boise, Idaho). Cell number was estimated for each well using Olympus CellSense Software from 3 random fields of view (area = 1.4 x 1.0 mm.). The average number of cells per field of view was 580. After images were captured, cells were lysed with 2 mM NaOH and lysate were transferred to 20 ml scintillation vials and mixed with UltimaGold scintillation fluid. Specific activity of [^{3}H] in each lysate was used to estimate glucose uptake, and specific activity of [^{14}C] in each lysate was used to estimate extracellular fluid volume using a Beckman-Coulter 1900 TA LC counter (Brea, CA). Specific activity of [^{3}H] 2-deoxyglucose in media was determined from three 10-µl aliquots mixed with 500-µl double-distilled water. All radioactive materials and scintillation fluids were purchased from Perkin-Elmer (Waltham, MA). Four technical replications per condition were performed and averaged for each animal.

Glucose Oxidation. Myoblasts plated on one side of sealable dual-well chambers were used to determine glucose oxidation. Wells were imaged using Olympus CellSense Software just before beginning the study. Three bright-field images per well were used to

estimate the number of cells per well. Cells were pre-incubated at 37ºC for 1 hour in treatment-spiked KHB media containing 0.1% BSA and 5 mM glucose and then washed at 37ºC for 20 minutes in glucose-free treatment-spiked KHB media containing 0.1% BSA. Chambers were then sealed using greased rubber gaskets and cells were incubated at 37º C for 2 hours in treatment-spiked gassed (95% O_2: 5% CO_2) KHB media and containing 5 mM [^{14}C-U] D-glucose (2.5 µCi/mmol) and 0.1% BSA. In the adjacent well of each sealed chamber, 2 mM NaOH was placed to capture CO_2 produced. After the incubation period, plates were cooled for 2 minutes at -20ºC, 2M HCl was injected into the media through the rubber seal to release bicarbonate-bound CO_2 from media and plates were incubated at 4ºC for 1 hour. Chambers were then opened and NaOH was collected and mixed with UltimaGold scintillation fluid in a 20-ml scintillation vial. Specific activity of $^{14}CO_2$ and media were determined as described above. Background was determined from no-cell control chambers, and leak tests were performed by measuring $^{14}CO_2$ in NaOH placed in adjacent chambers. Three technical replications per condition were averaged for each animal.

Statistical Analysis. Data were analyzed by ANOVA using the GLM procedure of SAS (SAS Institute, Cary, NC). Steer was the experimental unit (n=4). Rates were normalized to cell number and are expressed as percentage of basal rate (mean ± standard error). The mean for each experimental unit is the average of four and three technical replications for glucose uptake and glucose oxidation, respectively. Cell numbers were estimated from a minimum of 133 cells per well counted over a minimum of three random non-overlapping fields of view.

Results

Glucose Uptake. Incubation of myoblasts with insulin alone increased ($P < 0.05$) glucose uptake by ~40% compared to basal incubations (Figure 2). Incubation with β2 adrenergic agonist alone also increased ($P < 0.05$) glucose uptake by ~54% compared to basal. Conversely, incubation with β1 adrenergic agonist alone had no effect on glucose uptake compared to basal. Furthermore, glucose uptake in myoblasts that were co-incubated with β1 adrenergic agonist and insulin or with β2 adrenergic agonist and insulin was not different from myoblasts incubated with insulin alone.

Glucose Oxidation. Incubation of myoblasts with insulin alone increased ($P < 0.05$) glucose oxidation by ~68% compared to basal (Figure 3). Incubation with β2 adrenergic agonist alone also increased ($P < 0.05$) glucose oxidation by ~49% when compared to basal. Conversely, incubation with β1 adrenergic agonist alone had no effect on glucose oxidation. Furthermore, co-incubation with insulin and β1 agonist or with insulin and β2 agonist decreased glucose oxidation when compared to insulin alone. Incubation with β2 agonist alone increased glucose oxidation when compared to incubation with β1 agonist alone. In addition, co-incubation with insulin and β1 agonist was no different than co-incubation with insulin and β2 agonist.

Discussion

In this study, we show that glucose uptake and oxidation rates are increased when myoblasts are differentiated in the presence of β2 adrenergic stimulation when compared to β1 adrenergic stimulation or no stimulation. This indicates that β2-specific adrenergic activity increases glucose metabolic efficiency in differentiated myoblasts similar to its effects in skeletal muscle. Conversely, β2 adrenergic stimulation reduced insulin-stimulated glucose oxidation rates, which is opposite of the effect on skeletal muscle

during acute stimulation (Cadaret et al., 2017b). This indicates that the interaction between insulin and β agonists is different in myoblasts after sustained exposure during differentiation than it ultimately is in the mature fibers themselves. This difference could be due to sensitivity differences that exist between myoblasts and skeletal muscle or due to changes brought on by the longer exposure time in the present study.

Stimulation by β2 adrenergic agonist alone increased metabolic efficiency in myoblasts when compared to stimulation by β1 adrenergic agonist alone. We postulate that this is due to differences in metabolic pathways affected by each of these adrenergic agonists. Glucose oxidation was increased in myoblasts stimulated with the β2 adrenergic agonist, however, glucose oxidation was not affected by the β1 adrenergic agonist. This suggests that the β1 adrenergic agonist does not stimulate glucose oxidation and thus may be stimulating other metabolic pathways such as fatty acid mobilization in order to contribute to skeletal muscle gain efficiency observed in feedlot animals

In bovine myoblasts, β2 adrenergic stimulation decreased insulin-stimulated metabolic efficiency. However, stimulation of adult rat skeletal muscle with β2 adrenergic agonists and insulin increased insulin-stimulated metabolic efficiency (Cadaret et al., 2017b). This indicates that β2 agonist and insulin interactions in mature muscle fibers are not necessarily derived from the muscle stem cells. Furthermore, it is also important to note that the bovine myoblasts were chronically exposed to the β adrenergic stimulation since they were differentiated for 4 days in treatment-spiked media, whereas the adult rat skeletal muscle had only been acutely exposed (~4 hours) to the β adrenergic agonists. This could indicate that chronic exposure desensitizes β2

adrenergic receptors in differentiating myoblasts, thus contributing to the decrease in insulin-stimulated glucose oxidation.

Differentiation of myoblasts in the presence of β1 adrenergic agonist, had no effect on either glucose uptake or oxidation rates. This indicates that the β1 adrenergic agonist functions through different metabolic pathways than β2 adrenergic agonist to enhance muscle development and decrease lipid accumulation which may or may not involve changes in metabolic efficiency. However, β1 adrenergic stimulation reduced the ability of insulin to stimulate glucose oxidation. Chronic exposure to epinephrine is known to decrease insulin sensitivity (Deibert and Defronzo, 1980), and our findings would indicate that this is primarily due to β1 specific activity. Together, our findings demonstrate that zilpaterol HCl is more effective at increasing metabolic efficiency compared to ractopamine HCl, and that the beneficial effects of ractopamine HCl on muscle growth efficiency occur through some other physiological mechanism.

In conclusion, our study shows similarities as well as notable differences in responsiveness to β adrenergic stimulation between differentiated myoblasts and mature skeletal muscle. Most notably, β2 adrenergic stimulation had opposite effects on insulin-stimulated glucose oxidation in differentiated myoblasts in the present study as previously observed in mature skeletal muscle. This indicates that these interacting regulatory responses develop in the mature fiber and are not necessarily a phenotypic trait derived from muscle stem cells during fusion. Nevertheless, β2-stimulated glucose oxidation in our differentiated myoblasts paralleled stimulation in mature skeletal muscle, and β1 adrenergic stimulation had little to no effect on myoblasts, similar to our previous observations in skeletal muscle.

Differentiation Media		Constituents
1	Basal	DMEM + 2% FBS + 1% Ab/Am + 0.5% Gentamicin
2	Insulin	DMEM + 2% FBS + 1% Ab/Am + 0.5% Gentamicin + 5 mU/ml HumulinR
3	β1	DMEM + 2% FBS + 1% Ab/Am + 0.5% Gentamicin + 1 μM ractopamine HCl
4	β2	DMEM + 2% FBS + 1% Ab/Am + 0.5% Gentamicin + 0.05 μM zilpaterol HCl
5	β1 + Insulin	DMEM + 2% FBS + 1% Ab/Am + 0.5% Gentamicin + β1 + Insulin
6	β2 + Insulin	DMEM + 2% FBS + 1% Ab/Am + 0.5% Gentamicin + β2 + Insulin

Figure 1. Components of differentiation media for bovine myoblasts.

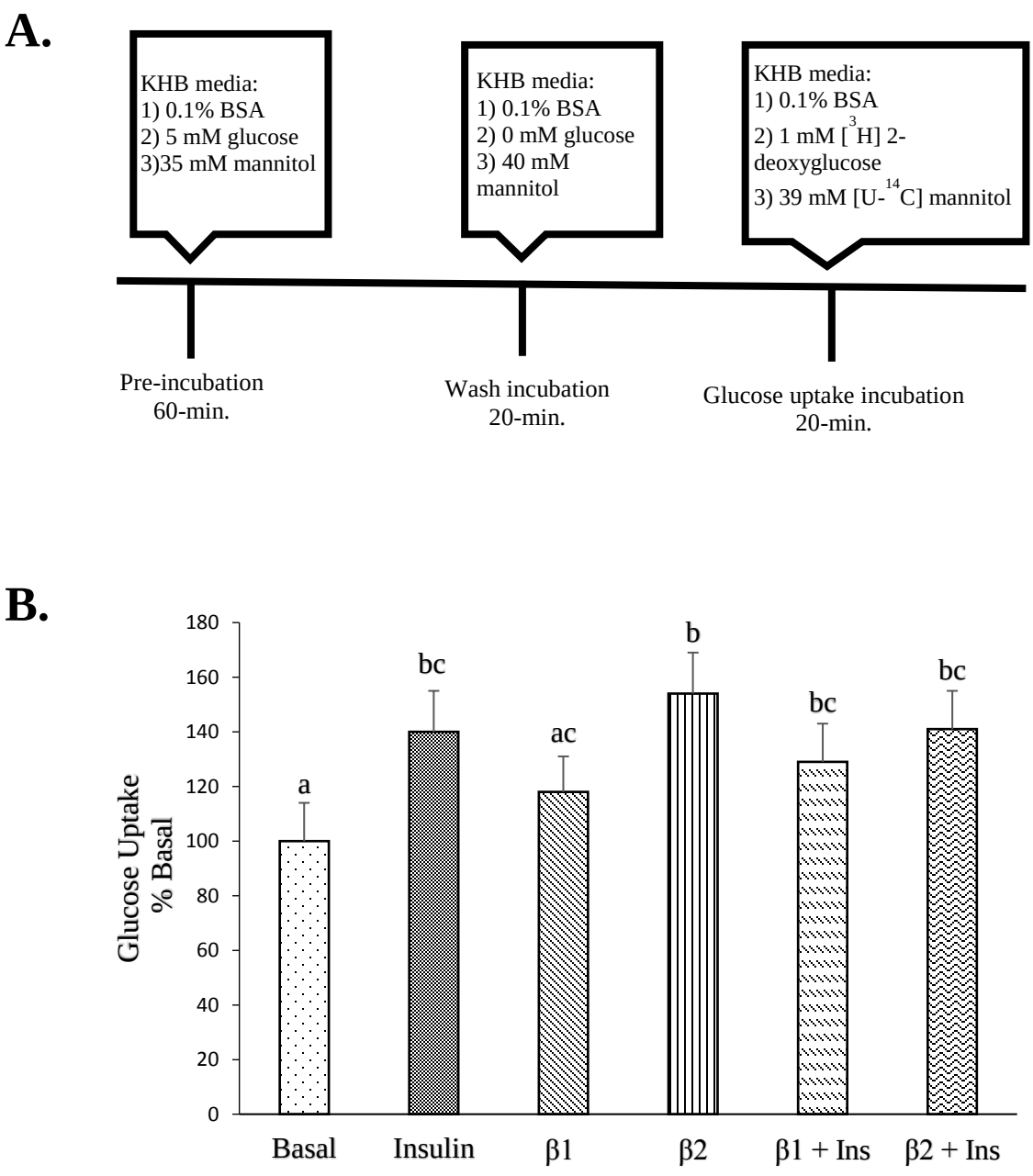

Figure 2. Schematic of glucose uptake study (A) and results of glucose uptake (B) in primary bovine myoblasts during 20 minute incubation after differentiation with one of the following treatments: No additive (basal), insulin (5 mU/ml HumulinR), β1 agonist (1 μM ractopamine HCl), β2 agonist (0.05 μM zilpaterol HCl), β1 agonist + insulin, or β2 agonist + insulin. ^{a,b,c} means with different superscripts differ ($P \leq 0.05$).

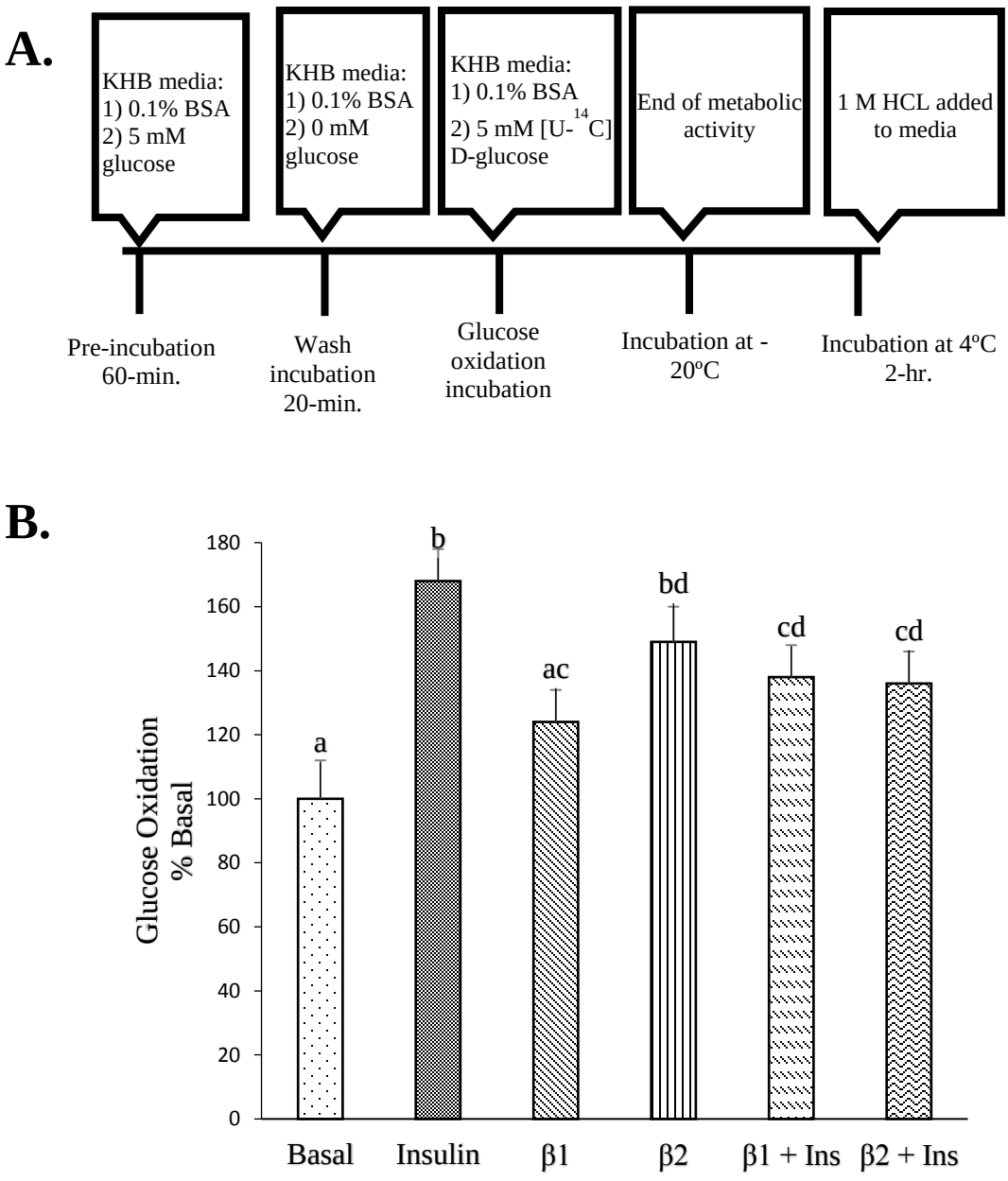

Figure 3. Schematic of glucose oxidation study (A) and results of glucose oxidation (B) in bovine myoblasts during a 120 minute incubation after differentiation with the following treatments: No additive (basal), insulin (5 mU/ml HumulinR), β1 agonist (1 μM ractopamine HCl), β2 agonist (0.05 μM zilpaterol HCl), β1 agonist + insulin, or β2 agonist + insulin. ^{a,b,c,d} means with different superscripts differ ($P \leq 0.05$).

Chapter 4

Oxidative capacity in myoblasts from high and low androstenedione cows

Abstract. Calves born to cows classified as having elevated follicular fluid concentrations of androstenedione (A4; High A4) have increased weaning weights compared to control Low A4 cows. However, the underlying mechanisms causing the increased weaning weights in calves born to High A4 cows is unknown. Our objective was to determine whether myoblasts isolated from High A4 cows had increased metabolic efficiency compared to myoblasts from Low A4 cows, which may help to explain the increase in weight gain in calves born to High A4 cows. For this study, myoblasts were isolated from the oblique of ten composite beef cows that were classified as having High (n=5; A4 ≥ 40 ng/ml) or Low (n=5; A4 ≤ 20 ng/ml) A4 concentrations. Myoblasts were incubated in complete growth media for 48 hours then incubated in treatment-spiked XF base medium containing either no additive (basal), 1 mU/ml insulin, or 10 mU/ml insulin. A mitochondrial stress test was performed on the myoblast cultures to measure oxygen consumption rate (OCR) as a proxy for mitochondrial respiration and extra-cellular acidification rate (ECAR) as a proxy for glycolysis. Serial injection of Oligomycin, FCCP, and Rotenone were utilized during the mitochondrial stress test to uncouple mitochondrial oxygen consumption and inhibit ATP production. This study showed no differences in mitochondrial respiration among A4 groups but a tendency for greater ($P = 0.1$) glycolysis in High A4 myoblasts incubated in basal conditions and in Low A4 myoblasts incubated with 1 mU/ml insulin. Moreover, OCR for basal respiration and for ATP production were greatest ($P < 0.05$) in the absence of insulin and were reduced similarly by 1 and 10 mU/ml insulin. Together, these results show that the

greater weaning weights in the High A4 population do not appear to be due to greater muscle metabolic efficiency.

Introduction

A population of cows within the University of Nebraska-Lincoln herd were classified as having high androstendione (A4) concentrations within their follicular fluid (Summers et al., 2014). Elevated concentrations of androgens is a hallmark of polycystic ovary syndrome (PCOS), which is known to decrease fertility rates (Franks, 2006). In fact, the cows identified as having High A4 concentrations had a 17% reduction in calving rates (Summers et al., 2014). Furthermore, elevated maternal androgen levels during gestation are known to impair fetal growth, leading to reduced birth weight (Carlsen et al., 2006), and lead to metabolic deficiencies into adult life (Smith et al., 2009). Interestingly, calves that were born to cows classified as having High A4 concentrations had greater weaning weights than calves born to Low A4 cows by 12 kg. (Summers et al., 2014). This indicates that metabolic adaptations to the physiological state of High A4 cows may be occurring during gestation. In addition to decreased fertility rates, a well characterized factor seen in patients with PCOS is altered metabolism leading to insulin resistance and obesity (Dunaif et al., 1989; Legro, 2000). We speculate that A4 may be acting in one of two ways. First, A4 may stimulate similar anabolic effects as testosterone, leading to an increase in skeletal muscle mass in the growing calf. Secondly, A4 may antagonize the effects of testosterone, and chronic in utero exposure to a High A4 environment may lead to a desensitization of skeletal muscle to A4, thus reducing its antagonist effect.

The mitochondrial electron transport chain consists of a series of redox reactions that reduce NADH using oxygen to form H_2O and ATP (Turrens and Boveris, 1980). There are 4 complexes within the electron transport chain in addition to an ATP synthase complex (Zhang et al., 1990). During a mitochondrial stress test, different compounds including Oligomycin, FCCP, and Rotenone are introduced into a cell culture sequentially to shut down complexes in the electron transport chain in order to measure specific components of oxygen consumption rate (OCR) (Figure1). Injection of Oligomycin into media blocks ATP synthesis by shutting down the ATP synthase complex of the electron transport chain (Nicholls et al., 2010). Consequentially, oxygen is maximally consumed by Complex IV. By measuring OCR before and after Oligomycin has been injected, the fraction of oxygen consumed during ATP synthesis and fraction needed to overcome proton leak can be determined. The second compound injected into the media is FCCP which uncouples ATP production, leading to rapid energy and oxygen consumption without the production of ATP. Thus, OCR and extra-cellular acidification rate (ECAR) increase because the cell will attempt to maintain energy balance by utilizing glycolysis for ATP generation. The last compound to be injected during the study is Rotenone, which inhibits Complex I. This shuts down the electron transport chain, inhibiting mitochondrial respiration and allowing both mitochondrial and non-mitochondrial fractions that contribute to respiration to be measured (Nicholls et al., 2010). By measuring OCR after each compound is added, cellular oxidation of total substrates (amino acids, lipids, and carbohydrates) can be determined. Furthermore, measurement of ECAR allows cellular glycolysis to be measured. The objective of this

study was to determine whether the increased weaning weights of the calves born to High A4 cows is a result of increased muscle metabolic efficiency in this population.

Materials and Methods

Animals. The following experiments were approved by the Institutional Animal Care and Use Committee at the University of Nebraska-Lincoln. Studies were conducted at the University of Nebraska-Lincoln Animal Science Complex which is accredited by the American Association for Accreditation of Laboratory Animal Care. Animals used for this study included ten composite beef cows [25% MARC III (25% Angus, 25% Hereford, 25% Pinzgauer, 25% Red Poll)].

Androstenedione Classification. Follicular fluid A4 concentrations were determined as previously described (Summers et al., 2014). Follicular fluid A4 concentrations were determined using a human A4 ELISA kit (Alpha Diagnostics International, San Antonio, TX). Inter- and intra- assay of variation for A4 coefficients were 6.5% and 5.7% respectively. The cows were classified as High (≥ 40 ng/ml A4) or Low (≤ 20 ng/ml) A4 based on dominant A4 concentration for follicle aspiration at ovariectomy procedures.

Myoblast Isolation. During ovariectomy, muscle from the oblique was collected and cleaned of all connective tissue and fat, and then finely minced. Minced muscle was placed 50 ml conical tubes, washed with ice-cold phosphate buffered saline (PBS, Fischer Bioreagents) and centrifuged at 1,500 x *g* for 5 minutes. Pelleted tissue was re-suspended in PBS, digested with protease type XIV from *Strept. griseus* (Sigma) at a concentration of 625 mg/500 ml PBS at 37ºC for 1 hour, and centrifuged at 1,500 x *g* for 5 minutes. Digested pellets were re-suspended in warm PBS and centrifuged 3 times at 500 x *g* for

10, 8, and 1 minute. Supernatant containing myoblasts was collected after each spin. These cells were incubated at 37ºC in pre-plate media (DMEM with 10% FBS) for 2 hours to remove fibroblasts. Cells were then re-suspended in freezing media (CGM + 10% dimethyl sulfoxide) and stored in liquid nitrogen. All media constituents were purchased from Sigma-Aldrich except insulin, which was purchased from Eli Lilly.

Cell Culture. Isolated bovine myoblasts were seeded onto 24-well XF^{e}24 Cell Culture Microplates (Seahorse Bioscience, North Billerica, MA) at an initial seeding density of 5,000 cells per well. Four background correction wells were seeded with no cells. Cells were grown as previously described (Yates et al., 2014) with some modifications. Briefly, all plates were coated with Poly-L-Lysine and Bovine Plasma Fibronectin. Cells were incubated at 37ºC and 5% CO_2 in complete growth media (78.5% DMEM, 20% FBS, 1% Ab/Am, and 0.5% Gentamicin) for 48 hours.

XF Assay Mito Stress Test. After 48 hour incubation in complete growth media, cells were washed twice with XF Base Media (Seahorse Bioscience) containing 25 mM glucose, 1.0 mM pyruvate, and 2 mM L-glutamine. The medium was then spiked with no additive (basal), 1 mU/ml insulin (Humulin-R), or 10 mU/ml insulin. 500 µl of XF Base Medium with the previously described additives were added to each well and cells were incubated at 37ºC in a non-CO_2 incubator for 1 hour. A cell mito stress test was run on the plate using the Seahorse XF-96 instrument (Seahorse Bioscience). 1.0 µM oligomycin, 1.0 µM FCCP, and 0.5 µM rotenone were sequentially injected to determine ATP-linked respiration, maximal respiration, and non-mitochondrial respiration, respectively. These parameters along with basal respiration were used to determine proton leak and respiration capacity.

BCA Protein Assay. Following the mito stress test, total protein of cells was determined in each well using a Pierce BCA Protein Assay Kit (Thermo Fisher, Waltham, MA). XF base media was aspirated from wells and 75 µl of RIPA buffer (Thermo Fisher) was added to each well. A sterile p200 pipette tip was used to scrape cells from the bottom of each well. 10 µl of each prepared serial dilution of albumin standard and each sample were added in triplicates to a 96-well plate followed by 200 µl of working solution. Plate was mixed thoroughly on a shaker for 30 seconds and incubated at 37ºC for 30 minutes. Absorbance was then measured at 562 nm on an EPOCH plate reader (Bio Tek, Winooski, VT) and analyzed using GEN5 software (Bio Tek).

Statistical Analysis. Data were analyzed using ANOVA output of SAS (SAS Institute, Cary, NC) as a 2x3 factorial. High vs. Low A4 was the main effect, and insulin concentration and A4*insulin interaction was in the subplot interaction. Cow was the experimental unit (N=10). The mean for each experimental unit is the average of 6 technical replications per insulin concentration for OCAR and ECAR. For each well, OCR and ECAR were normalized to amount of total protein. Means for each measurement period are the average of three measurements taken 5 minutes apart. Data are presented as means ± standard error.

Results

For this study, OCR (Figure 2) was measured in bovine myoblasts. There were not differences among A4 groups for basal respiration rate, ATP production, or maximal ATP production for OCR (Figure 3). Similarly, there were not differences among A4 groups for any measurements taken after each inhibitory compound was injected into the

media for OCR. In addition, ECAR (Figure 4) was measured and there were not differences among A4 groups for glycolytic capacity (Figure 5). However, the myoblasts from High A4 cows incubated at basal and Low A4 cows incubated with 1 mU/ml of insulin tended to have increased ($P = 0.1$) glycolysis after injection of Oligomycin. There were no differences among treatments for any other measurements taken after FCCP or Rotenone were injected into the media for ECAR.

Discussion

In this study, we did not find any differences in OCR between myoblasts isolated from High A4 and Low A4 cows, suggesting that mitochondrial respiration and thus ATP production from oxidation is similar between High and Low A4 cows. Furthermore, myoblasts from High A4 cows in the absence of insulin and myoblasts from Low A4 cows in the presence of insulin had a tendency for increased glycolytic rates.

The OCR between the High and Low A4 cows was similar, indicating that cellular oxygen consumption rate among treatments was not different. Since oxygen is being consumed at a similar rate among treatments, it suggests that carbohydrates, amino acids, and lipids are being oxidized at similar rates. Furthermore, the addition of inhibitory compounds such as Oligomycin, FCCP, and Rotinone had similar affects among treatments which also suggests that oxidation rates are not different among groups. Adaptations occurring during gestation or other growth advantages that lead to increased weaning weights in High A4 cattle populations are likely not derived from enhanced metabolic efficiency in muscle from the cow.

A major role of insulin in metabolism is to stimulate uptake of glucose into cells where it can be metabolized by one of several pathways, including anaerobic glycolysis.

The treatments had similar glycolytic capacities but myoblasts from High A4 cows in the absence of insulin and Low A4 cows when insulin was present had a tendency for increased glycolytic rates. This was determined by increased acidification in cell media resulting from lactate production, a byproduct of glycolysis.

We hypothesized that myoblasts from the High A4 cows would have increased metabolic efficiency compared to myoblasts from the Low A4 cows which would help to explain greater pre-weaning growth in this population. However, we saw no differences in skeletal muscle oxidative metabolic efficiency. This suggests that the increased weaning weights seen in the calves from cows classified as High A4 is due to a different molecular mechanism than postulated. However, additional studies that take a closer look at the metabolic efficiency of the skeletal muscle from the calves themselves may help clarify gaps in our understanding of the underlying mechanism that leads to their increased weaning weights.

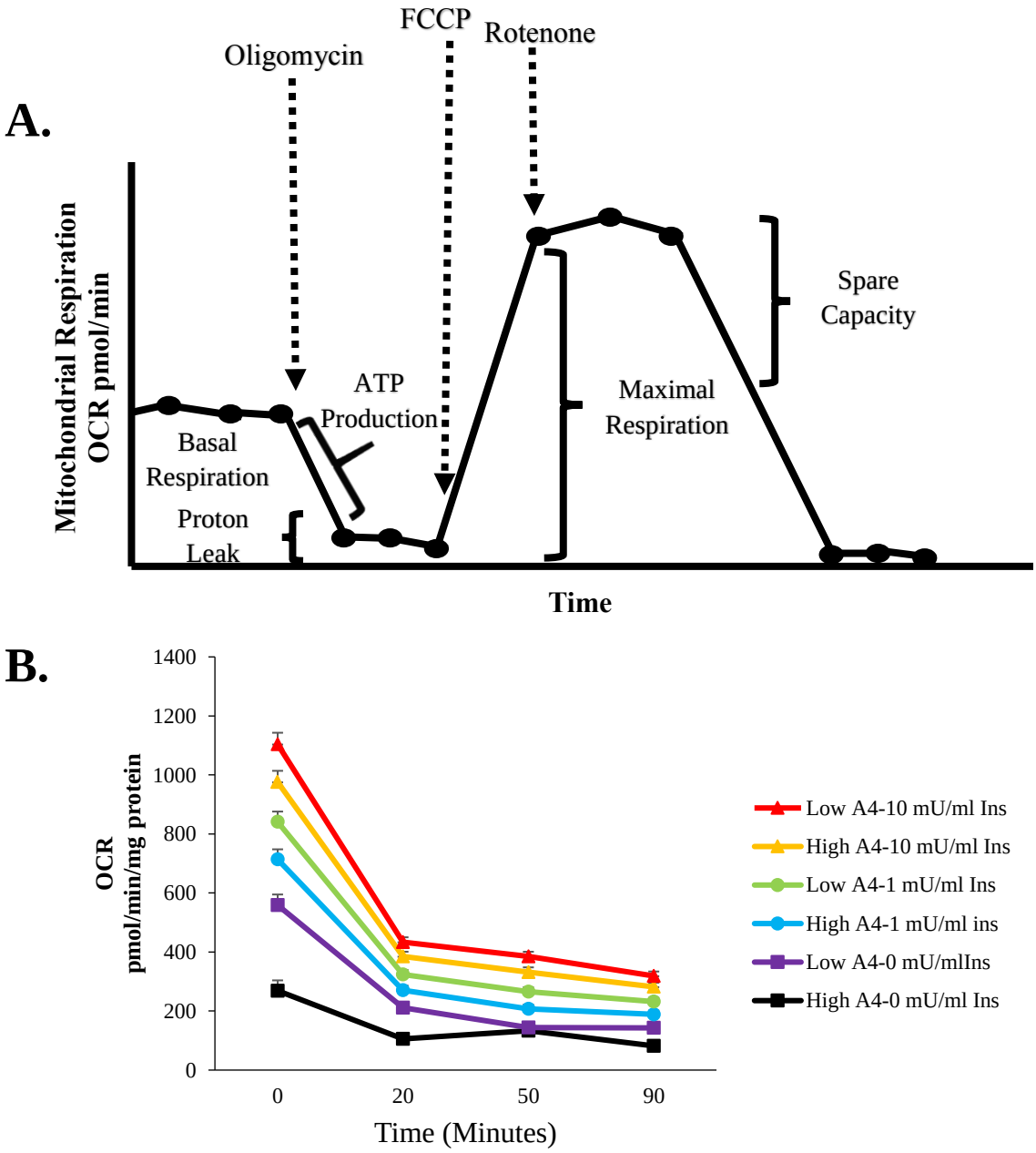

Figure 1. Components of mitochondrial respiration (A). Oxygen consumption rate in bovine myoblasts from High and Low A4 cows incubated with either basal, 1 mU/ml, or 10 mU/ml of insulin. Each mean is the average of three measurements taken during the period (B).

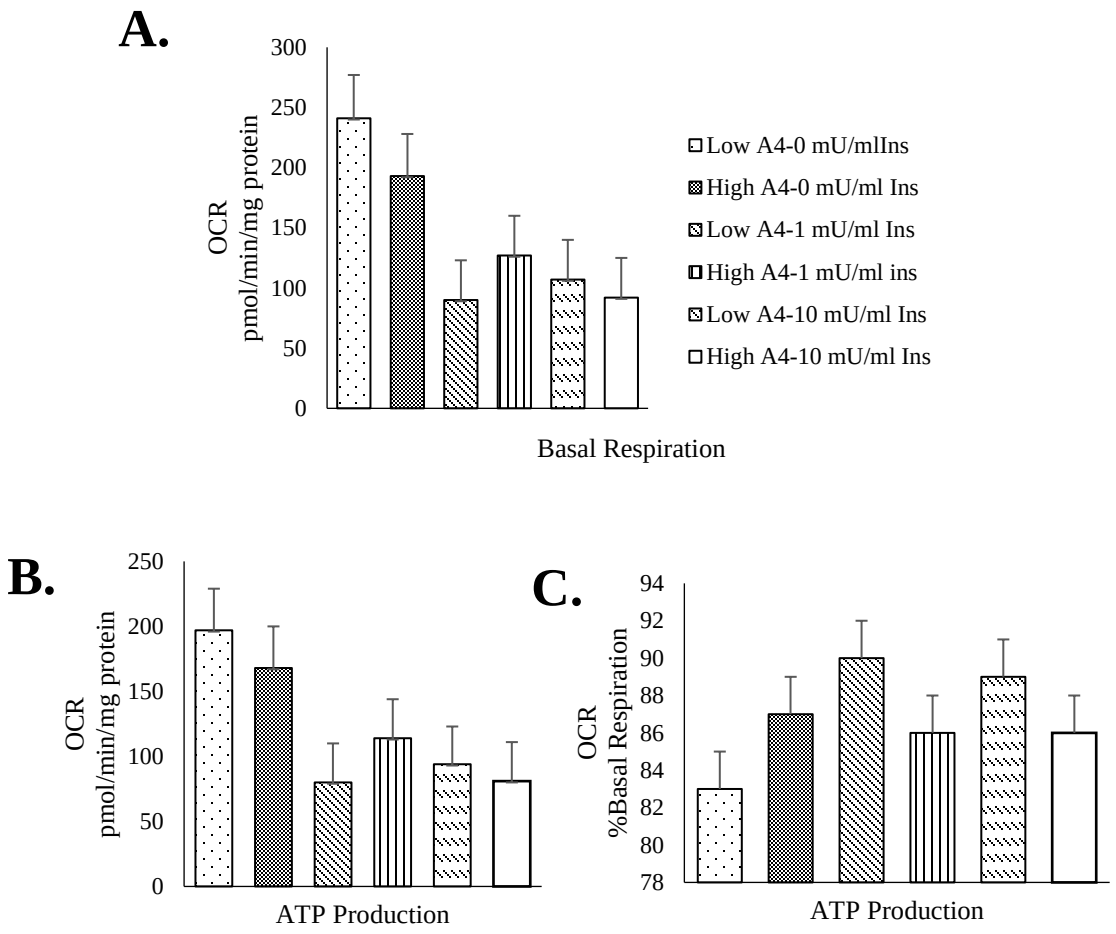

Figure 3. Oxygen consumption for basal respiration (A), ATP production (B), and ATP production normalized to basal (C) in bovine myoblasts from High and Low A4 cows incubated with either basal, 1 mM/ml, or 10 mM/ml of insulin.

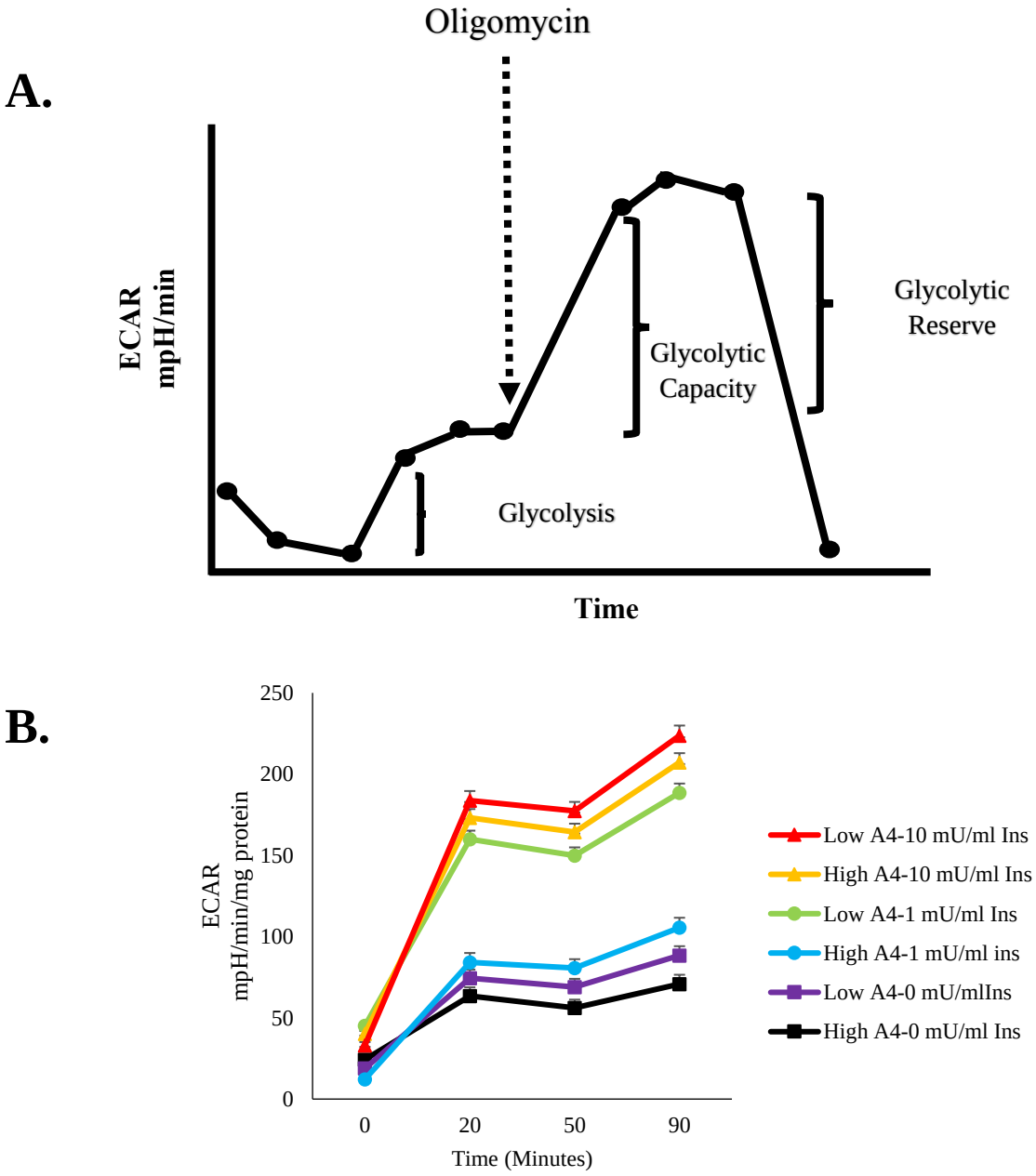

Figure 4. Components of glycolysis (A) and extra-cellular acidification (ECAR) rates in bovine myoblasts from High and Low A4 cows incubated with either basal, 1 mU/ml, or 10 mU/ml of insulin (B).

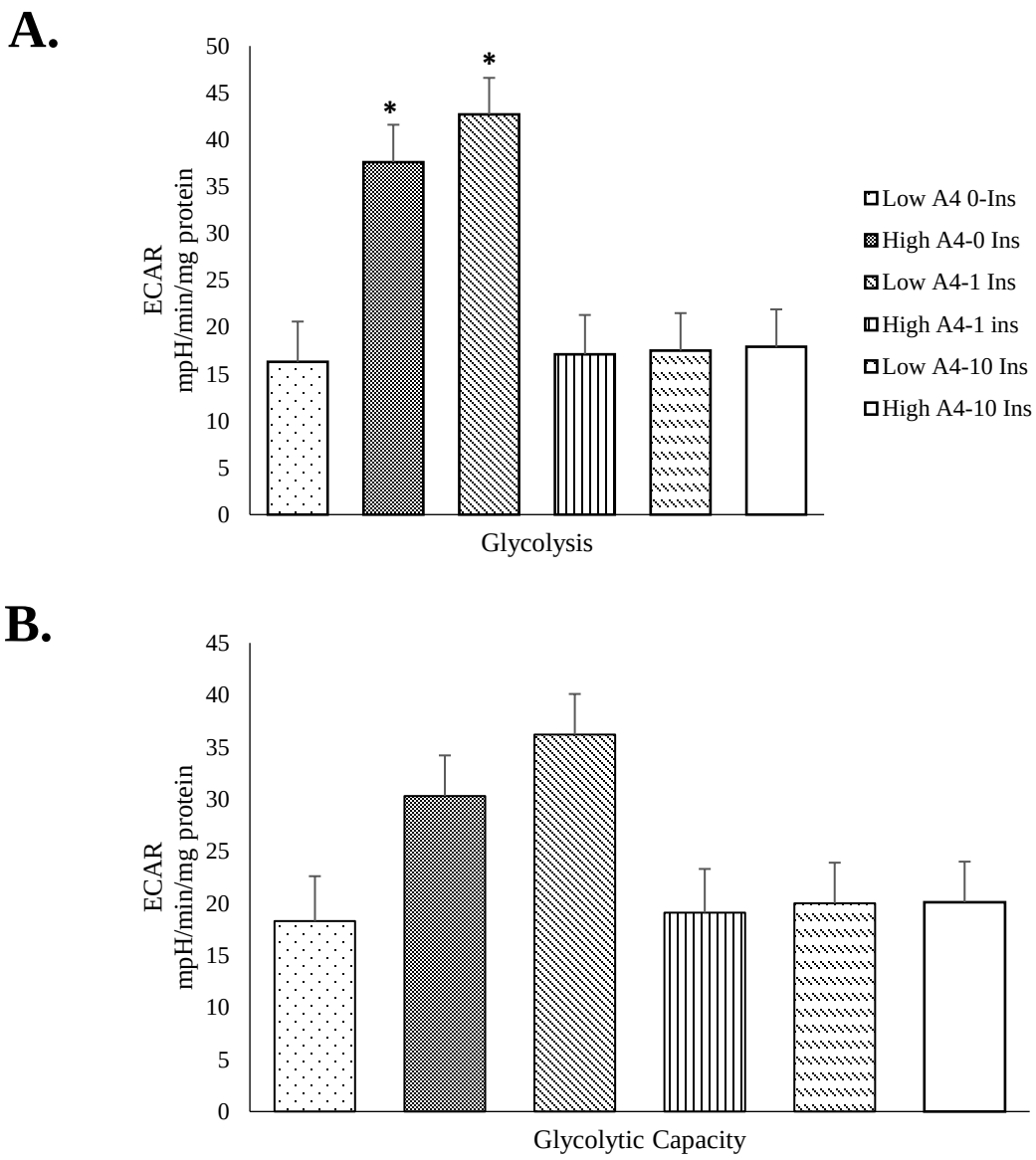

Figure 5. Glycolysis (A) and glycolytic capacity (B) in bovine myoblasts from High and Low A4 cows incubated with either basal, 1 mU/ml, or 10 mU/ml of insulin. *Means tend to differ ($P \leq 0.10$) between A4 groups within insulin concentrations.

References

Abbott, D., D. Barnett, C. Bruns, and D. Dumesic. 2005. Androgen excess fetal programming of female reproduction: a developmental aetiology for polycystic ovary syndrome? Human reproduction update 11: 357-374.

Abel, E. D. et al. 2001. Adipose-selective targeting of the GLUT4 gene impairs insulin action in muscle and liver. Nature 409: 729-733.

Alisi, A., N. Panera, C. Agostoni, and V. Nobili. 2011. Intrauterine growth retardation and nonalcoholic Fatty liver disease in children. International journal of endocrinology 2011.

Allen, R. E., and L. K. Boxhorn. 1989. Regulation of skeletal muscle satellite cell proliferation and differentiation by transforming growth factor- beta, insulin- like growth factor I, and fibroblast growth factor. Journal of cellular physiology 138: 311-315.

Allen, R. E., R. A. Merkel, and R. B. Young. 1979. Cellular aspect of muscle growth: myogenic cell proliferation. Journal of Animal Science 49: 115-127.

Allen, R. E., and L. L. Rankin. 1990. Regulation of satellite cells during skeletal muscle growth and development. Proceedings of the Society for Experimental Biology and Medicine 194: 81-86.

Andersen, H. J., N. Oksbjerg, J. F. Young, and M. Therkildsen. 2005. Feeding and meat quality–a future approach. Meat science 70: 543-554.

Barker, D. J. et al. 1993. Type 2 (non-insulin-dependent) diabetes mellitus, hypertension and hyperlipidaemia (syndrome X): relation to reduced fetal growth. Diabetologia 36: 62-67.

Barker, D. J., K. L. Thornburg, C. Osmond, E. Kajantie, and J. G. Eriksson. 2010. The surface area of the placenta and hypertension in the offspring in later life. The International journal of developmental biology 54: 525.

Barker, D. J. P. 1998. Mothers, babies, and health in later life. Elsevier Health Sciences.

Barnes, T. L. et al. 2017. Identifying hyperthermia in heat-stressed lambs and its effects on β agonist–stimulated glucose oxidation in muscle. ASAS Western Section: 106.

Barry, J. S., and R. V. Anthony. 2008. The pregnant sheep as a model for human pregnancy. Theriogenology 69: 55-67.

Bartha, J. L., R. Romero- Carmona, and R. Comino- Delgado. 2003. Inflammatory cytokines in intrauterine growth retardation. Acta obstetricia et gynecologica Scandinavica 82: 1099-1102.

Bauer, M. et al. 1998. Fetal growth and placental function. Molecular and cellular endocrinology 140: 115-120.

Bell, A., R. Wilkening, and G. Meschia. 1987. Some aspects of placental function in chronically heat-stressed ewes. Journal of developmental physiology 9: 17-29.

Brodsky, D., and H. Christou. 2004. Current concepts in intrauterine growth restriction. Journal of Intensive Care Medicine 19: 307-319.

Brown, L. D. 2014. Endocrine regulation of fetal skeletal muscle growth: impact on future metabolic health. Journal of Endocrinology 221: R13-R29.

Brown, L. D. et al. 2015. Limited capacity for glucose oxidation in fetal sheep with intrauterine growth restriction. American Journal of Physiology-Regulatory, Integrative and Comparative Physiology 309: R920-R928.

Cadaret, C. N. et al. 2017a. Maternal inflammation at mid-gestation in pregnant rats impairs fetal muscle growth & development at term. ASAS Western Section: 213.

Cadaret, C. N., K. A. Beede, H. E. Riley, and D. T. Yates. 2017b. Acute exposure of primary rat soleus muscle to zilpaterol HCl (β2 adrenergic agonist), TNFα, or IL-6 in culture increases glucose oxidation rates independent of the impact on insulin signaling or glucose uptake. Cytokine 96: 107-113.

Cantor, B., T. Tyler, R. Nelson, and G. Stein. 1980. Oligohydramnios and transient neonatal anuria: a possible association with the maternal use of prostaglandin synthetase inhibitors. The Journal of reproductive medicine 24: 220-223.

Carlsen, S., G. Jacobsen, and P. Romundstad. 2006. Maternal testosterone levels during pregnancy are associated with offspring size at birth. European Journal of Endocrinology 155: 365-370.

Cefalu, W. T. 2001. Insulin resistance: cellular and clinical concepts. Experimental biology and medicine 226: 13-26.

Centner, T., J. Alvey, and A. Stelzleni. 2014. Beta agonists in livestock feed: Status, health concerns, and international trade. Journal of animal science 92: 4234-4240.

Chiswick, M. L. 1985. Intrauterine growth retardation. British medical journal (Clinical research ed.) 291: 845.

Cotechini, T., W. Hopman, and C. Graham. 2014. Inflammation-induced fetal growth restriction in rats is associated with altered placental morphometrics. Placenta 35: 575-581.

Dandona, P., A. Aljada, A. Chaudhuri, P. Mohanty, and R. Garg. 2005. Metabolic syndrome a comprehensive perspective based on interactions between obesity, diabetes, and inflammation. Circulation 111: 1448-1454.

De Blasio, M. J., K. L. Gatford, J. S. Robinson, and J. A. Owens. 2007. Placental restriction of fetal growth reduces size at birth and alters postnatal growth, feeding activity, and adiposity in the young lamb. American Journal of Physiology-Regulatory, Integrative and Comparative Physiology 292: R875-R886.

DeFronzo, R. et al. 1981. The effect of insulin on the disposal of intravenous glucose: results from indirect calorimetry and hepatic and femoral venous catheterization. Diabetes 30: 1000-1007.

Deibert, D. C., and R. A. Defronzo. 1980. Epinephrine-induced insulin resistance in man. Journal of Clinical Investigation 65: 717.

Dionne, M. S., L. N. Pham, M. Shirasu-Hiza, and D. S. Schneider. 2006. Akt and FOXO dysregulation contribute to infection-induced wasting in Drosophila. Current Biology 16: 1977-1985.

Dulloo, A. G. 2008. Thrifty energy metabolism in catch-up growth trajectories to insulin and leptin resistance. Best practice & research Clinical endocrinology & metabolism 22: 155-171.

Dunaif, A., K. R. Segal, W. Futterweit, and A. Dobrjansky. 1989. Profound peripheral insulin resistance, independent of obesity, in polycystic ovary syndrome. Diabetes 38: 1165-1174.

Dunlop, K., M. Cedrone, J. F. Staples, and T. R. Regnault. 2015. Altered Fetal Skeletal Muscle Nutrient Metabolism Following an Adverse In Utero Environment and the Modulation of Later Life Insulin Sensitivity. Nutrients 7: 1202-1216.

Duvnjak, L., T. Bulum, and Z. Metelko. 2008. Hypertension and the metabolic syndrome. Diabetologia Croatica 37: 83-89.

Edmondson, D. G., and E. N. Olson. 1989. A gene with homology to the myc similarity region of MyoD1 is expressed during myogenesis and is sufficient to activate the muscle differentiation program. Genes & development 3: 628-640.

Eisner, J. R., D. A. Dumesic, J. W. Kemnitz, and D. H. Abbott. 2000. Timing of prenatal androgen excess determines differential impairment in insulin secretion and action in adult female rhesus monkeys. The Journal of Clinical Endocrinology & Metabolism 85: 1206-1210.

Faloia, E. et al. 2004. Body composition, fat distribution and metabolic characteristics in lean and obese women with polycystic ovary syndrome. Journal of endocrinological investigation 27: 424-429.

Franks, S. 1995. Polycystic ovary syndrome. N Engl j med 1995: 853-861.

Franks, S. 2006. Diagnosis of polycystic ovarian syndrome: in defense of the Rotterdam criteria. The Journal of Clinical Endocrinology & Metabolism 91: 786-789.

Galan, H. L. et al. 1999. Relationship of fetal growth to duration of heat stress in an ovine model of placental insufficiency. American journal of obstetrics and gynecology 180: 1278-1282.

Gallagher, E. J., D. LeRoith, and E. Karnieli. 2011. The metabolic syndrome—from insulin resistance to obesity and diabetes. Medical Clinics of North America 95: 855-873.

Gatford, K., R. Simmons, M. De Blasio, J. Robinson, and J. Owens. 2010. Review: placental programming of postnatal diabetes and impaired insulin action after IUGR. Placenta 31: S60-S65.

Gillespie, M. A. et al. 2009. p38-γ–dependent gene silencing restricts entry into the myogenic differentiation program. The Journal of cell biology 187: 991-1005.

Gluckman, P. D., and M. A. Hanson. 2004. Living with the past: evolution, development, and patterns of disease. Science 305: 1733-1736.

Green, A. S. et al. 2011. Characterization of glucose-insulin responsiveness and impact of fetal number and sex difference on insulin response in the sheep fetus. American Journal of Physiology-Endocrinology and Metabolism 300: E817-E823.

Greenwood, P., and A. Bell. 2002. Consequences of intra-uterine growth retardation for postnatal growth, metabolism and pathophysiology. Reproduction (Cambridge, England) Supplement 61: 195-206.

Grounds, M. D., and Z. Yablonka-Reuveni. 1993. Molecular and cell biology of skeletal muscle regeneration Molecular and cell biology of muscular dystrophy. p 210-256. Springer.

Grundy, S. M. 2000. Metabolic complications of obesity. Endocrine 13: 155-165.

Hales, C. et al. 1991. Fetal and infant growth and impaired glucose tolerance at age 64. Bmj 303: 1019-1022.

Hales, C. N., and D. J. Barker. 1992. Type 2 (non-insulin-dependent) diabetes mellitus: the thrifty phenotype hypothesis. Diabetologia 35: 595-601.

Hales, C. N., and D. J. Barker. 2001. The thrifty phenotype hypothesis. British medical bulletin 60: 5-20.

Hay, W. W. 2006. Recent observations on the regulation of fetal metabolism by glucose. The Journal of physiology 572: 17-24.

Heinig, J. et al. 2000. Determination of cytokine mRNA-expression in term human placenta of patients with gestational hypertension, intrauterine growth retardation and gestational diabetes mellitus using polymerase chain reaction. Zentralblatt für Gynäkologie 122: 413-418.

Holcberg, G. et al. 2001. Increased production of tumor necrosis factor-α TNF-α by IUGR human placentae. European Journal of Obstetrics & Gynecology and Reproductive Biology 94: 69-72.

Hotamisligil, G. S., N. S. Shargill, and B. M. Spiegelman. 1993. Adipose Expression of Tumor Necrosis Factor- : Direct Role in Obesity-Linked Insulin Resistance. SCIENCE-NEW YORK THEN WASHINGTON- 259: 87-87.

Hutcheson, D. A., J. Zhao, A. Merrell, M. Haldar, and G. Kardon. 2009. Embryonic and fetal limb myogenic cells are derived from developmentally distinct progenitors and have different requirements for β-catenin. Genes & development 23: 997-1013.

Inskip, H. et al. 2007. Size at birth and its relation to muscle strength in young adult women. Journal of internal medicine 262: 368-374.

Irshad, A. et al. 2013. Factors influencing carcass composition of livestock: A review. J. Anim. Prod. Adv 3: 177-186.

James, D. E., R. Brown, J. Navarro, and P. F. Pilch. 1988. Insulin-regulatable tissues express a unique insulin-sensitive glucose transport protein.

Jones, C., and J. Ritchie. 1978. The metabolic and endocrine effects of circulating catecholamines in fetal sheep. The Journal of physiology 285: 395-408.

Kitabchi, A. E., G. E. Umpierrez, J. M. Miles, and J. N. Fisher. 2009. Hyperglycemic crises in adult patients with diabetes. Diabetes care 32: 1335-1343.

Klasing, K. C., and B. J. Johnstone. 1991. Monokines in growth and development. Poultry Science 70: 1781-1789.

Klein, S. et al. 2007. Waist circumference and cardiometabolic risk: a consensus statement from shaping America's health: Association for Weight Management and Obesity Prevention; NAASO, the Obesity Society; the American Society for Nutrition; and the American Diabetes Association. Obesity 15: 1061-1067.

Klip, A., and M. R. Pâquet. 1990. Glucose transport and glucose transporters in muscle and their metabolic regulation. Diabetes care 13: 228-243.

Kupferminc, M. J., A. M. Peaceman, T. R. Wigton, K. A. Rehnberg, and M. L. Socol. 1994. Tumor necrosis factor-α is elevated in plasma and amniotic fluid of patients with severe preeclampsia. American journal of obstetrics and gynecology 170: 1752-1759.

L'honore, A. et al. 2007. Identification of a new hybrid serum response factor and myocyte enhancer factor 2-binding element in MyoD enhancer required for MyoD expression during myogenesis. Molecular biology of the cell 18: 1992-2001.

Law, C. et al. 2002. Fetal, infant, and childhood growth and adult blood pressure a longitudinal study from birth to 22 years of age. Circulation 105: 1088-1092.

Lean, I. J., J. M. Thompson, and F. R. Dunshea. 2014. A meta-analysis of zilpaterol and ractopamine effects on feedlot performance, carcass traits and shear strength of meat in cattle. PloS one 9: e115904.

Legro, R. S. 2000. The genetics of obesity Lessons for polycystic ovary syndrome. Annals of the New York Academy of Sciences 900: 193-202.

Leney, S. E., and J. M. Tavaré. 2009. The molecular basis of insulin-stimulated glucose uptake: signalling, trafficking and potential drug targets. Journal of Endocrinology 203: 1-18.

Leos, R. A. et al. 2010. Chronic exposure to elevated norepinephrine suppresses insulin secretion in fetal sheep with placental insufficiency and intrauterine growth restriction. American Journal of Physiology-Endocrinology and Metabolism 298: E770-E778.

Li, D.-K., L. Liu, and R. Odouli. 2003. Exposure to non-steroidal anti-inflammatory drugs during pregnancy and risk of miscarriage: population based cohort study. Bmj 327: 368.

Lillioja, S. et al. 1987. Skeletal muscle capillary density and fiber type are possible determinants of in vivo insulin resistance in man. Journal of Clinical Investigation 80: 415.

Limesand, S. W., P. J. Rozance, D. Smith, and W. W. Hay. 2007. Increased insulin sensitivity and maintenance of glucose utilization rates in fetal sheep with placental insufficiency and intrauterine growth restriction. American Journal of Physiology-Endocrinology and Metabolism 293: E1716-E1725.

Maeda, T., and B. J. Koos. 2009. Adenosine A 1 and A 2a receptors modulate insulinemia, glycemia, and lactatemia in fetal sheep. American Journal of Physiology-Regulatory, Integrative and Comparative Physiology 296: R693-R701.

Marconi, A. M., C. L. Paolini, G. Zerbe, and F. C. Battaglia. 2006. Lactacidemia in intrauterine growth restricted (IUGR) pregnancies: relationship to clinical severity, oxygenation and placental weight. Pediatric research 59: 570-574.

Marette, A., Y. Liu, and G. Sweeney. 2014. Skeletal muscle glucose metabolism and inflammation in the development of the metabolic syndrome. Reviews in Endocrine and Metabolic Disorders 15: 299-305.

Mersmann, H. J. 1998. Overview of the effects of beta-adrenergic receptor agonists on animal growth including mechanisms of action. Journal of animal science 76: 160-172.

Molteni, R., S. Stys, and F. Battaglia. 1978. Relationship of fetal and placental weight in human beings: fetal/placental weight ratios at various gestational ages and birth weight distributions. The Journal of reproductive medicine 21: 327-334.

Morrison, J. L. 2008. Sheep models of intrauterine growth restriction: fetal adaptations and consequences. Clinical and Experimental Pharmacology and Physiology 35: 730-743.

Nicholls, D. G. et al. 2010. Bioenergetic profile experiment using C2C12 myoblast cells. Journal of visualized experiments: JoVE.

Østensen, M. 1996. Safety of non-steroidal anti-inflammatory drugs during pregnancy and lactation. Inflammopharmacology 4: 31-41.

Ozanne, S. et al. 2005. Low birthweight is associated with specific changes in muscle insulin-signalling protein expression. Diabetologia 48: 547-552.
Pickup, J., and M. Crook. 1998. Is type II diabetes mellitus a disease of the innate immune system? Diabetologia 41: 1241-1248.
Pollack, R. N., and M. Y. Divon. 1992. Intrauterine growth retardation: definition, classification, and etiology. Clinical obstetrics and gynecology 35: 99-107.
Reaven, G. M. 2005. The insulin resistance syndrome: definition and dietary approaches to treatment. Annu. Rev. Nutr. 25: 391-406.
Regnault, T. et al. 2007. Development and mechanisms of fetal hypoxia in severe fetal growth restriction. Placenta 28: 714-723.
Rinaudo, P., and E. Wang. 2012. Fetal programming and metabolic syndrome. Annual review of physiology 74: 107.
Rumack, C. M. et al. 1981. Neonatal intracranial hemorrhage and maternal use of aspirin. Obstet Gynecol 58: 52S-56S.
Saltiel, A. R., and C. R. Kahn. 2001. Insulin signalling and the regulation of glucose and lipid metabolism. Nature 414: 799-806.
Schultz, E. 1989. Satellite cell behavior during skeletal muscle growth and regeneration. Medicine and science in sports and exercise 21: S181-186.
Sir-Petermann, T. et al. 2002. Maternal serum androgens in pregnant women with polycystic ovarian syndrome: possible implications in prenatal androgenization. Human reproduction 17: 2573-2579.
Smith, P., T. L. Steckler, A. Veiga-Lopez, and V. Padmanabhan. 2009. Developmental programming: differential effects of prenatal testosterone and dihydrotestosterone on follicular recruitment, depletion of follicular reserve, and ovarian morphology in sheep. Biology of reproduction 80: 726-736.
Späte, U., and P. C. Schulze. 2004. Proinflammatory cytokines and skeletal muscle. Current Opinion in Clinical Nutrition & Metabolic Care 7: 265-269.
Spranger, J. et al. 2003. Inflammatory cytokines and the risk to develop type 2 diabetes results of the prospective population-based European Prospective Investigation into Cancer and Nutrition (EPIC)-Potsdam Study. Diabetes 52: 812-817.
Steckler, T., J. Wang, F. F. Bartol, S. K. Roy, and V. Padmanabhan. 2005. Fetal programming: prenatal testosterone treatment causes intrauterine growth retardation, reduces ovarian reserve and increases ovarian follicular recruitment. Endocrinology 146: 3185-3193.
Strydom, P. 2016. Performance-enhancing technologies of beef production. Animal Frontiers 6: 22-30.
Summers, A. F. et al. 2014. Altered theca and cumulus oocyte complex gene expression, follicular arrest and reduced fertility in cows with dominant follicle follicular fluid androgen excess. PloS one 9: e110683.
Turrens, J. F., and A. Boveris. 1980. Generation of superoxide anion by the NADH dehydrogenase of bovine heart mitochondria. Biochemical Journal 191: 421-427.
Tuuli, M. G., A. Cahill, D. Stamilio, G. Macones, and A. O. Odibo. 2011. Comparative efficiency of measures of early fetal growth restriction for predicting adverse perinatal outcomes. Obstetrics & Gynecology 117: 1331-1340.

Uysal, K. T., S. M. Wiesbrock, M. W. Marino, and G. S. Hotamisligil. 1997. Protection from obesity-induced insulin resistance in mice lacking TNF-α function. Nature 389: 610-614.

Vaag, A. 2009. Low birth weight and early weight gain in the metabolic syndrome: consequences for infant nutrition. International Journal of Gynecology & Obstetrics 104: S32-S34.

Van Antwerp, D. J., S. J. Martin, T. Kafri, D. R. Green, and I. M. Verma. 1996. Suppression of TNF-alpha-induced apoptosis by NF-kB. Science 274: 787.

van Gelder, M. M., N. Roeleveld, and H. Nordeng. 2011. Exposure to non-steroidal anti-inflammatory drugs during pregnancy and the risk of selected birth defects: a prospective cohort study. PLoS One 6: e22174.

Van Itallie, T. B. 1985. Health implications of overweight and obesity in the United States. Annals of internal medicine 103: 983-988.

Vonnahme, K. 2012. How the maternal environment impacts fetal and placental development: implications for livestock production. Animal Reproduction 9: 789-797.

Wilson, S., J. McEwan, P. Sheard, and A. Harris. 1992. Early stages of myogenesis in a large mammal: formation of successive generations of myotubes in sheep tibialis cranialis muscle. Journal of Muscle Research & Cell Motility 13: 534-550.

Wood, I. S., and P. Trayhurn. 2003. Glucose transporters (GLUT and SGLT): expanded families of sugar transport proteins. British Journal of Nutrition 89: 3-9.

Yates, D. et al. 2012. Developmental programming in response to intrauterine growth restriction impairs myoblast function and skeletal muscle metabolism. Journal of pregnancy 2012.

Yates, D. T. et al. 2016. Intrauterine growth-restricted sheep fetuses exhibit smaller hindlimb muscle fibers and lower proportions of insulin-sensitive Type I fibers near term. American Journal of Physiology-Regulatory, Integrative and Comparative Physiology 310: R1020-R1029.

Yates, D. T., X. Chen, and S. W. Limesand. 2011. Environmental heat stress impairs placental function, fetal growth and development, and postnatal performance in livestock. Environmental Physiology of Livestock: 209.

Yates, D. T. et al. 2014. Myoblasts from intrauterine growth- restricted sheep fetuses exhibit intrinsic deficiencies in proliferation that contribute to smaller semitendinosus myofibres. The Journal of physiology 592: 3113-3125.

Ylihärsilä, H. et al. 2007. Birth size, adult body composition and muscle strength in later life. International journal of obesity 31: 1392-1399.

Zammit, P. S. et al. 2006. Pax7 and myogenic progression in skeletal muscle satellite cells. Journal of cell science 119: 1824-1832.

Zhang, J.-M., and J. An. 2007. Cytokines, inflammation and pain. International anesthesiology clinics 45: 27.

Zhang, Y., O. Marcillat, C. Giulivi, L. Ernster, and K. Davies. 1990. The oxidative inactivation of mitochondrial electron transport chain components and ATPase. Journal of Biological Chemistry 265: 16330-16336.

Zhu, M.-J., S. P. Ford, P. W. Nathanielsz, and M. Du. 2004. Effect of maternal nutrient restriction in sheep on the development of fetal skeletal muscle. Biology of reproduction 71: 1968-1973.

Zhu, M. J. et al. 2006. Maternal nutrient restriction affects properties of skeletal muscle in offspring. The Journal of physiology 575: 241-250.